REGULATION OF THE TUMOR SUPPRESSOR *ARF* BY TGFB IN HUMAN CANCER CELLS

APPROVED BY SUPERVISORY COMMITTEE

Stephen X. Skapek, MD

Rolf A. Brekken, PhD

Jerry W. Shay, PhD

Pier P. Scaglioni, MD

This work is dedicated to:

My parents, without whom I would not be the person I am today.

My mentor, who took a chance on me when I was between a rock and a hard place.

My family, who have always been so proud of me even when I doubted myself.

My friends, who let me in and shared part of themselves with me.

My committee, whose patience and understanding run deeps.

All those I have met, talked to, and learned about. When science couldn’t quench my thirst for understanding in life, even a brief conversation with a stranger was often an enlightening and uplifting moment.

REGULATION OF THE TUMOR SUPPRESSOR *ARF* BY TGFB IN HUMAN CANCER CELLS

by

JARED COLE HOOKS

DISSERTATION

Presented to the Faculty of the Graduate School of Biomedical Sciences

The University of Texas Southwestern Medical Center at Dallas

In Partial Fulfillment of the Requirements

For the Degree of

DOCTOR OF PHILOSOPHY

The University of Texas Southwestern Medical Center at Dallas

Dallas, Texas

December, 2016

REGULATION OF THE TUMOR SUPPRESSOR *ARF* BY TGFB IN HUMAN CANCER CELLS

Jared Cole Hooks, Ph.D

The University of Texas Southwestern Medical Center at Dallas, 2016

Stephen X. Skapek, M.D

Since its discovery, $p14^{ARF}$ ($p19^{Arf}$ in mice) has been shown to be an important regulator of the cell cycle, carrying out this function through p53-dependent and independent mechanisms. *ARF* expression has recently been shown by the Skapek lab to be induced by TGFβ in mouse embryonic fibroblast and HeLa cells. TGFβ itself has been well characterized for its role as a "dual-edged sword," acting as a tumor suppressor or oncogene depending on the context. Though preliminary work has looked at the basic connections between TGFβ pathway components and their necessity for induction of *ARF*, many open questions remain, especially in translating findings from mouse to human cells. For my dissertation research, I have chosen to further investigate the regulation of TGFβ-driven induction of *ARF*. The knowledge gained through understanding TGFβ-dependent regulation of *ARF* is important in understanding disease progression and could also provide new avenues for cancer treatment through restoration of the TGFβ pathway to harness the tumor suppressive effects of $p14^{ARF}$.

PRIOR PUBLICATIONS

Hooks, J.C., Matharage, J.P., and Udugamasooriya, D.G. (2011). Development of homomultimers and heteromultimers of lung cancer-specific peptoids. Biopolymers *96*, 567-577.

TABLE OF CONTENTS

LIST OF FIGURES

LIST OF TABLES

LIST OF APPENDICES

CHAPTER 1:

Introduction

The Alternative Reading Frame (*ARF*) of *CDKN2A*

A search for genes whose deletion was responsible for different forms of melanoma traced to the 9p21 region subsequently led to the discovery of the first cyclin-dependent kinase inhibitor (*CDKN2A*) (Cowan et al., 1988; Fountain et al., 1992; Petty et al., 1993; Serrano et al., 1993). Using a yeast two hybrid screen probing for protein-protein interactions with CDK4 as bait, the group screened a cDNA library and found a positive hit for a 16 kD protein, which they termed $p16^{INK4}$ (inhibitor of CDK4). They went on to show that ectopic addition of $p16^{INK4}$ extract inhibited a fusion protein of retinoblastoma protein (Rb) in a reconstituted system containing active CDK4/cyclin D complexes. This inhibition was specific for CDK4/cyclin D complexes as a system containing CDK2/cyclin D2 showed no inhibition of Rb when $p16^{INK4}$ extract was added.

Though it was hypothesized that $p16^{INK4}$ acted as a negative regulator of cell growth through inhibition of Rb, its role as a tumor suppressor was still unknown. It had been shown that different cancer types harbored frequent alterations of the 9p21 locus, suggesting that loss of $p16^{INK4}$ could contribute to cancer progression. (Cheng et al., 1993; Diaz et al., 1990; Diaz et al., 1988; Fountain et al., 1992; James et al., 1993; Lukeis et al., 1990; Merlo et al., 1994; Middleton et al., 1991; Olopade et al., 1993; Olopade et al., 1992; van der Riet et al., 1994). Using 100 melanoma cell lines and sequence tagged sites (STSs) covering the 9p21 locus, a region encompassing two gene encoding regions were shown to be deleted in over half of the cell line panel (Kamb et al., 1994). One gene was shown to encode $p16^{INK4}$ using sequence homology and both genes were shown to be deleted in various cell lines representing many different types of cancer using STSs in or around both genes. The second gene was later shown to encode $p15^{INK4B}$, a protein that acts in the same manner of as $p16^{INK4A}$ by inhibiting CDK4/6-dependent Rb phosphorylation (Hannon and Beach, 1994).

Upon further investigation of transcripts encoding $p16^{INK4A}$, two different forms were found in humans and mice that shared exons 2 and 3, but had separate starting exons termed exon 1α and 1β (Stone et al., 1995). Exon 1β was shown to have a different reading frame and promoter than exon 1α and thus was termed alternative reading frame (*ARF*). The *ARF* gene was found to encode a 19 kD, 169 amino acid protein in mice and 14 kD, 132 amino acid protein in humans, respectively referred to as $p19^{ARF}$ and $p14^{ARF}$ (Quelle et al., 1995; Stott et al., 1998).

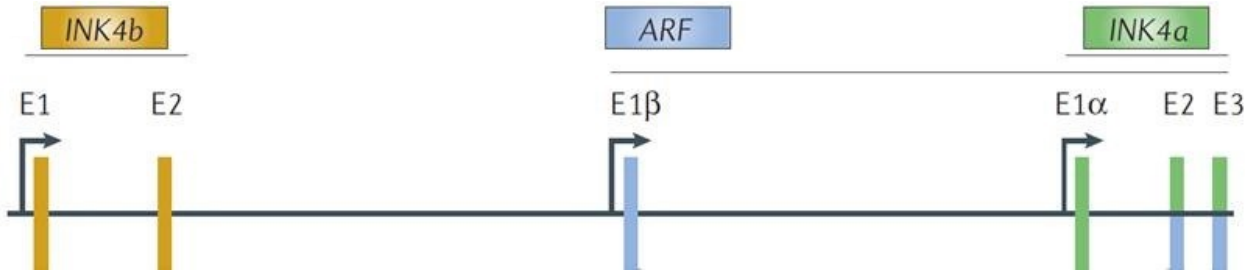

Figure 1.1: Schematic diagram representing the *CDKN2A*/*ARF*/*CDKN2B* locus. The locus contains three genes (*CDKN2A*, *ARF*, and *CDKN2B*) expressing three different proteins ($p16^{INKa}$, $p14^{ARF}$, and $p15^{INK4b}$, respectively). *CDKN2A* and *ARF* share exons 2 and 3, but differ in the first exon (exon 1α and exon 1β, respectively) whose expression is controlled independently by separate promoters (modified from Sherr, 2006).

Though *ARF* was believed to be important in some capacity due to conservation in mice and the intimate association with $p16^{INK4A}$, there was no definitive evidence until $p19^{arf}$ was cloned by the Sherr lab (Quelle et al., 1995). Using mouse erythroleukemia cell lines, cDNA of $p19^{Arf}$ was cloned and then inserted into a retrovirus vector for ectopic expression. After incubating NIH 3T3 cells - which lack Ink4a - with the $p19^{Arf}$ expressing retrovirus, cell cycle arrest was induced at both G1 and G2/M stages. In addition, $p19^{Arf}$ did not associate with CDKs from NIH 3T3 lysates and CDK/Cyclin complexes expressed in insect Sf9 cells retained their

enzymatic ability, indicating that $p19^{Arf}$-induced cell cycle arrest was mechanistically different from that of $p16^{Ink4a}$.

The tumor suppressive effects of $p19^{Arf}$ independent of $p16^{Ink4a}$ became apparent upon observation of tumor development early in the life of mice which had exon 1β of *Arf* replaced with the neomycin resistance gene but exon 1α was left intact (Kamijo et al., 1997). In addition to this, mouse embryonic fibroblasts (MEFs) able to escape replicative senescence upon repeated passaging were shown to have either lost expression of $p19^{Arf}$ or have mutated p53 indicating the mutual exclusivity of *Arf* and p53 required for growth arrest. Furthermore, ectopic expression of $p19^{Arf}$ in cell lines lacking functional p53 resisted the growth inhibitory effects of *Arf*, hinting at the possibility that it acts upstream of p53.

Inactivation of the *CDKN2A*/*ARF* locus through point mutations or deletions occur in many human cancers but many of these events occur in either exon 1α or in exon 2 (Hall and Peters, 1996; Hirama and Koeffler, 1995; Kamb et al., 1994; Nobori et al., 1994; Pollock et al., 1996; Quelle et al., 1997). To what extent *ARF* contributed to tumorigenesis in these cases was unknown as the impact on its function as a tumor suppressor was not clear. To resolve this, 6 independent, commonly occurring point mutations and one independent, 2 amino acid deletion in a highly conserved region were made in exon 2 of either mouse $p16^{Ink4a}$ or $p19^{Arf}$ cDNA (Quelle et al., 1997). Mutations know to affect $p16^{Ink4a}$ function did in fact affect its ability to cause cell cycle arrest when ectopically expressed in NIH 3T3 cells, though the same alterations did not impede the growth inhibition properties of $p19^{Arf}$. When different exons of $p19^{Arf}$ were expressed ectopically, it was found that nearly all of the growth repressive effects were retained in exon 1β.

The first clear evidence of a mechanism of cell cycle arrest for *ARF* came when Zhang et al. demonstrated the ability of $p14^{ARF}$ to bind MDM2, an E3 ubiquitin-protein ligase that inhibits p53 by targeting it for degradation (Zhang et al., 1998). Using a yeast two-hybrid screen with $p14^{ARF}$ as bait and a two-hybrid cDNA library from HeLa cells, the researchers detected binding of the C-terminus of MDM2 to $p14^{ARF}$. This interaction was also confirmed using *in vitro* ectopic expression and immunoprecipitation of both proteins in HeLa and COS7 cells. Consistent with previous research showing that the majority of $p19^{Arf}$ growth inhibitory action lies in exon 1β, MDM2 was shown to bind to the first exon of $p14^{ARF}$ and that this interaction led to a reduction in MDM2 stabilization as determined by pulse-chase in which MDM2's half-life was reduced from 90 min to 30 min when coexpressed with $p14^{ARF}$. This mechanism was also confirmed for the mouse protein $p19^{ARF}$ (Pomerantz et al., 1998). Thus, a major component of *ARF*'s tumor suppressor activity was determined to be the indirect activation of p53 through targeted degradation of MDM2.

At this point, it was clear that *ARF* could act as an oncogenic sensor as it had been shown that expression of Ras, Myc, or E2F1 resulted in increased expression of *ARF* which led to increased p53 levels (Bates et al., 1998; Palmero et al., 1998; Zindy et al., 1998). But in addition to its p53-dependent tumor suppressive activity, there was evidence that *ARF* could act independently of p53 to cause cell cycle arrest. It was shown that mice with knockouts of *Arf* and *p53* develop a wider range of tumor from different tissues along with multiple primary tumors, independent of Mdm2, as opposed to inactivation of *Arf* or *p53* alone (Weber et al., 2000). Furthermore, G1 cell cycle arrest occurred upon ectopic expression of $p19^{Arf}$ in triple knockout MEFs (but not *p53* and *Arf* double knockout MEFs), demonstrating that *Arf* could influence the cell cycle outside of the Mdm2-p53 pathway.

In addition to its ability to induce *ARF* expression, the transcription factor E2F1 was the first protein identified to be directly regulated by *ARF* (Eymin et al., 2001). Researchers found that not only was endogenous $p14^{ARF}$ and E2F1 able to physically interact, ectopic expression of $p14^{ARF}$ in Saos2 cells (which express high levels of E2F1) co-transfected with a luciferase reporter driven by an E2F1-dependent promoter resulted in significant reduction of luciferase activity, demonstrating the ability of *ARF* to inhibit E2F1-dependent transcription. Interestingly, the group also found that MDM2 co-precipitated with $p14^{ARF}$/E2F1 complexes. Using the same reporter as before, they showed that in *Mdm2/p53* double knockout MEFs co-transfection of *ARF* with E2F1 did not inhibit E2F1 transcription but upon addition of MDM2, inhibition was rescued.

Concurrent with the discovery of E2F1/$p14^{ARF}$ interaction, c-MYC was also identified as a direct target of $p14^{ARF}$ using co-IPs in HeLa cells, which are effectively p53-null as it is targeted for degradation by the HPV protein E6 (Qi et al., 2004). This group found that $p19^{Arf}$ mainly bound to the C-terminal helix-loop-helix/leucine zipper domain, which is required for c-Myc to heterodimerize with Max to form a transcriptional activator complex, and the N-terminal transcriptional regulatory domain, the latter of which exhibited the most binding. In MEFs that were *p53*- and *Arf*-null, induced c-Myc expression resulted in increased levels of c-Myc regulated genes such as tert and cdk4 whereas MEFs that were only *p53*-null (which results in high $p19^{Arf}$ expression) did not show increased expression of these genes.

Since this time, there has been work looking for different binding partners of *ARF* and its contribution to cellular senescence (reviewed in Sherr, 2006, 2012). The fundamentals for *ARF* though, from its discovery as coding a unique protein that shares exons with *CDKN2A*, to its participation in cell cycle arrest through various mechanisms and interactions, were established by these researchers.

Transforming Growth Factor Beta (TGFβ)

The initial discovery of TGFβ was during the characterization of a growth factor secreted from cells transformed using sarcoma virus that had the ability to transform and promote the growth of “normal” cells in soft agar, giving it the moniker sarcoma growth factor or SGF (de Larco and Todaro, 1978). Upon further purification of SGF, two separate fractions retained transformation activity in the presence of epidermal growth factor (EGF) giving rise to TGFα and TGFβ, the latter of which showed much more activity (Anzano et al., 1982; Roberts et al., 1981). It was known by this time that TGFβ was present in normal cells and that it participated in many processes, including wound healing, by promoting the formation of collagen and angiogenesis, and surprisingly growth inhibition (Roberts et al., 1986; Sporn et al., 1983; Tucker et al., 1984). This was the beginning of TGFβs history in cancer biology of being a double-edged sword, a molecule able to intricately regulate cell growth in most normal contexts but act as a strong oncogene in many cancers.

There are 3 different TGFβ ligands (1, 2, and 3) that can all act by the same mechanism of binding as a dimer to TGFβ receptors (TGFβRI and II) as seen in figure 1.2. Upon ligand binding and activation of the resulting receptor complex, an R-SMAD (SMAD2 and SMAD3) is recruited to the receptors, phosphorylated, and released. Activated R-SMAD can then bind to the co-SMAD, SMAD4, which then translocates to the nucleus and functions as a transcriptional regulator through recruitment of different cofactors. This process is commonly known as the canonical TGFβ-signaling pathway as it is the primary mode in which TGFβ ligands act to regulate TGFβ-responsive genes. Disruptions or alterations in this pathway at key points during cancer development and progression can switch TGFβ from tumor suppressor to oncogene.

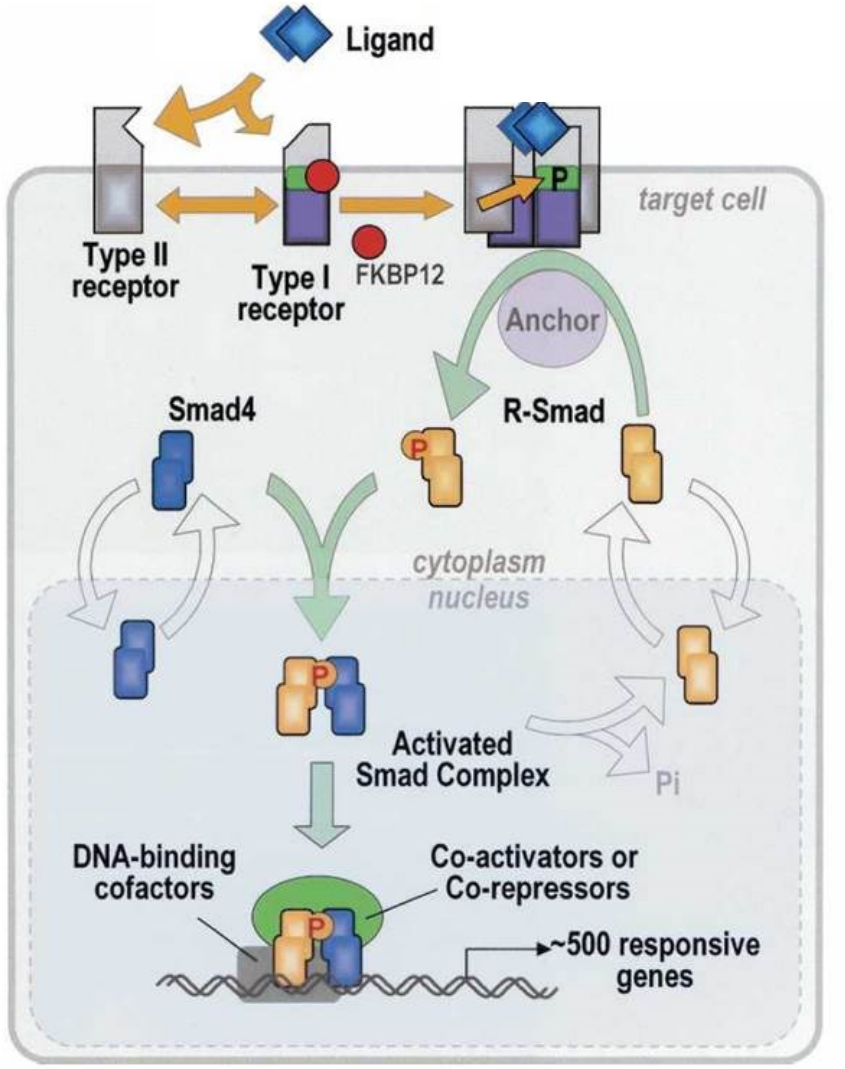

Figure 1.2: Schematic diagram of the TGFβ-SMAD signaling pathway. A general overview of the TGFβ signaling showing activated, dimeric ligand (TGFβ) binding to type I and II TGFβ receptors. FKBP12, an inhibitor of the type I receptor that prevents dimerization is released and the active heterodimeric receptor is formed. The type II receptor phosphorylates the type I receptor, allowing receptor SMADs (R-SMAD) to bind with assistance of an anchoring ligand. The R-SMAD is phosphorylated allowing association with the co-Smad (SMAD4) which facilitates translocation to the nucleus. The SMAD complex recruits and binds with other cofactors at SMAD binding elements (SBE) within the DNA, facilitating activation or repression of TGFβ responsive genes (modified from Massague et al., 2005).

TGFβ-dependent Regulation of *ARF*

The link between *ARF* and TGFβ was discovered in the Skapek lab while investigating *Arf*'s role in the developing mouse eye. It was found that $Arf^{-/-}$ mice had smaller eyes than wildtype mice with phenotypes very similar to the eye disease persistent hyperplastic primary vitreous (PHPV) in humans (McKeller et al., 2002). Upon histological examination of the eyes, it was clear that the hyaloid vascular system (HVS), which precedes the development of mature vasculature in the eye, had failed to regress. This phenotype was not replicated in mice lacking p53 or Cdkn2a, indicating that this was a p53-independent function of *Arf* (Martin et al., 2004). In transgenic mice where exon 1β of *Arf* had been replaced with *Gfp, Arf* promoter activation could be detected in perivascular cells (which expressed markers mainly associated with pericyte cells) before HVS regression would normally occur. Using this mouse model, activation of the *Arf* promoter was found to begin at E12.5 of embryonic development and colocalized with Pdgfrβ, an important factor in supporting development of normal vasculature by recruiting perivascular cells (Silva et al., 2005)). In *Pdgfrβ/Arf* double knockout mice, regression of the perivascular cells were rescued showing that *Arf* acts upstream of Pdgfrβ in the normal development of the mouse eye.

Interestingly, it had previously been shown that $Tgfβ2^{-/-}$ mice developed similar characteristics of PHPV leading to the hypothesis that Tgfβ2 played a role in *Arf*'s repression of Pdgfrβ (Saika et al., 2001; Sanford et al., 1997). Upon incubation of wildtype MEFs for 72 hr with 5ng/mL of Tgfβ2, western blotting showed that $p19^{Arf}$ levels increased significantly and repeating this experiment in the presence of the TGFβRI inhibitor SB431542 blunted this induction along with pSmad2 levels (Freeman-Anderson et al., 2009). To test the dependence of *Arf* induction *in vivo*, a transgenic mouse line in which exon 1β had been replaced *LacZ* (Fig. 1.3A) was crossed with a hetero- or homozygous *Tgfβ2* knockout mouse line. At E13.5, X-gal

staining of *Tgfβ2*$^{-/-}$ mouse embryo eyes showed low *LacZ* expression as compared to the *Tgfβ2*$^{+/-}$ background (Fig 1.3B). Furthermore, *Arf*$^{LacZ/+}$ MEFs showed robust increases in β-gal activity when treated with Tgfβ2 or Tgfβ1 (Fig 1.3C). These experiments demonstrated a unique mode of *Arf* induction dependent upon Tgfβ signaling both *in vitro* and *in vivo*.

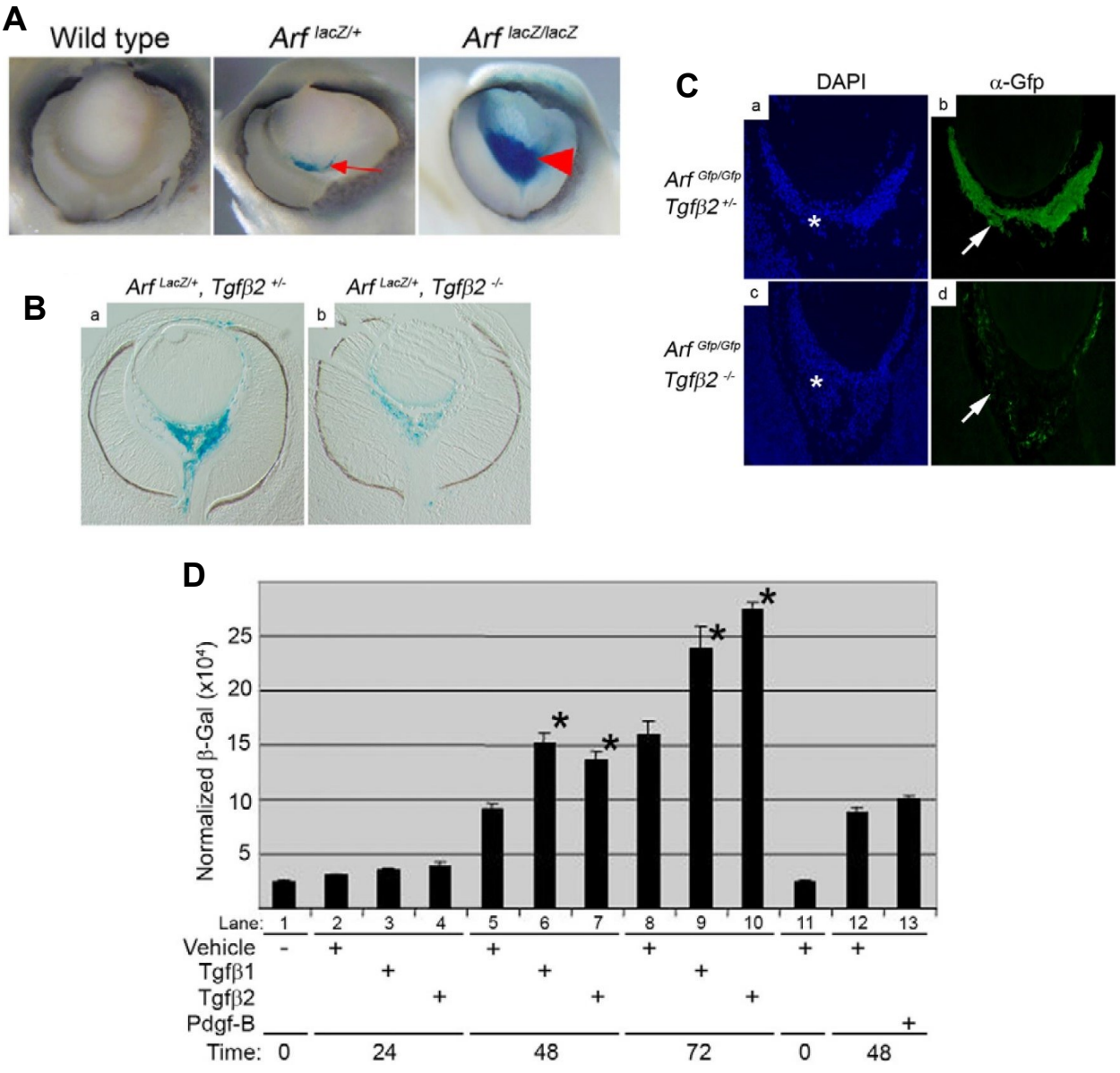

Figure 1.3: Dependency of *Arf* expression by Tgfβ in the developing mouse eye and MEFs. A) Transgenic mice with either one or both copies *Arf* exon 1β replaced with lacZ show increased expressed of the transgene in the primary vitreous at E13.5. B & C) In mice which are null for *Tgfβ2*, the expression of the transgene is blunted. D) Both Tgfβ1 and 2 can elicit *Arf* induction in MEFs harvested from wildtype mice (modified from Freeman-Anderson et al., 2009).

To determine the components downstream of the activated Tgfβ receptor complex necessary for induction, Smad6 was ectopically expressed in *Arf*$^{LacZ/LacZ}$ MEFs. Upon 48 hr incubation with Tgfβ2, cells expressing Smad6 did not show increase in β-gal activity when compared to wildtype MEFs. Inhibition of Smad2 and Smad3 by target siRNA also blocked Tgfβ-dependent p19^{Arf} induction in wildtype MEFs (Zheng et al., 2010). Interestingly, when chromatin immunoprecipitation (ChIP) was used to determine the presence of Smad2/3 near the *Arf* promoter, binding could be detected within 1.5 hr of Tgfβ2 treatment. Two sites with the highest signal were identified approximately -1200 and -35 bp transcriptionally upstream of the start site henceforth referred to as distal and proximal, respectively . While this established the role of canonical Tgfβ signaling, it was also found that activation of p38 contributed as p19^{Arf} levels were reduced upon targeted p38 inhibition, demonstrating the importance of a non-canonical pathway.

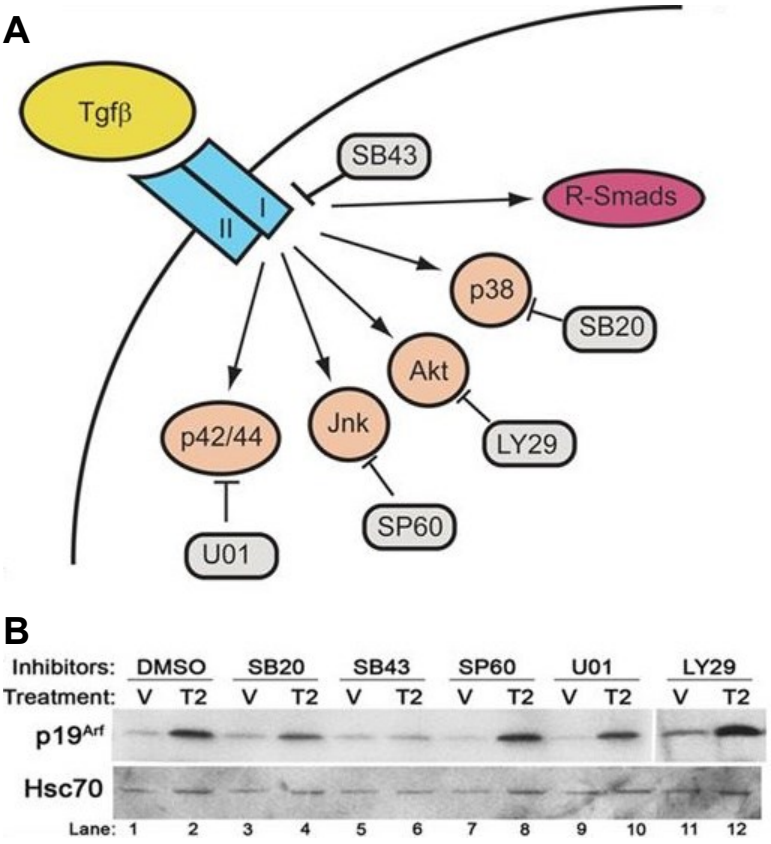

Figure 1.4: Both r-SMADs and p38 affect *Arf* induction in response to TGFβ. A) Non-canonical downstream signaling mediators (beige) of the TGFβ pathway and the small molecule inhibitors (gray) used to block their activation. B) Western blot showing changes in p19^{Arf} induction in response to Tgfβ2 and in response to different inhibitors. The Tgfβr-I inhibitor SB43 ablates p19^{Arf} induction in response to Tgfβ2 while the p38 inhibitor SB20 significantly decreases induction (modified from Freeman-Anderson et al., 2009).

It was also established that Tgfβ-dependent *Arf* induction was not isolated to mice. In a panel of cancer cells, the HeLa cell line was found to induce $p14^{ARF}$ in response to TGFβ1 (Zheng unpublished). In addition, both the timeframe of increased *ARF* expression and the contribution of p38 to its induction were consistent with previous finding in MEFs.

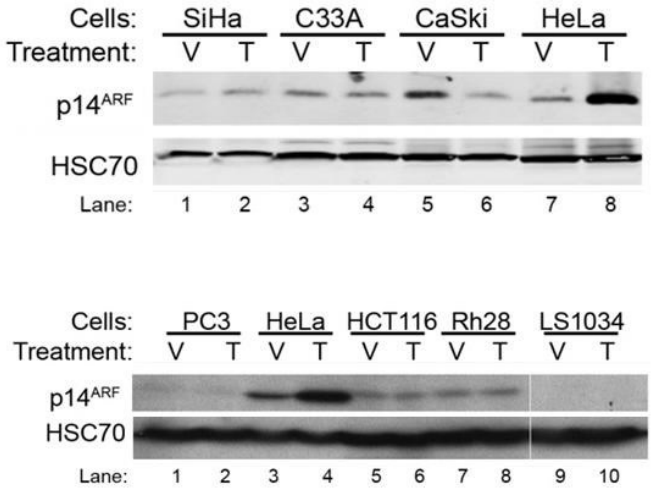

Figure 1.5: HeLa shows TGFβ-dependent induction of *ARF*. In two groups of cancer cells from different origins, HeLa was shown to induce $p14^{ARF}$ in response to TGFβ1, demonstrating that this phenomenon can occur in human cells in addition to MEFs (Zheng, unpublished).

Building upon these discoveries, two important questions presented themselves about ARFs role as a tumor suppressor in response to TGFβ: how is *ARF* regulated at a transcriptional level in response to TGFβ and how do these previous findings in mice translate to human cancer? For my dissertation, I designed experiments to answer certain aspects of these questions based upon recent data by the Skapek lab and others. In my second chapter, I will attempt to answer whether a Tgfβ-responsive distant, *cis*-acting enhancer of *Arf* exists in region previously shown to participate in the repression of *Arf*. Next, building upon initial observations from the Skapek lab that HeLa cells induce $p14^{ARF}$ in a TGFβ-dependent manner, my third chapter will focus on what components of the previously outlined signaling pathway are necessary, and translate these findings to a focused panel of lung cancer cells. For my fourth chapter, I will address the transcriptional regulation directly at the *ARF* promoter by asking how POLR2A recruitment changes in response to TGFβ.

CHAPTER 2:

Distal Cis-acting Enhancers of *ARF* in the Human 9p21.3 Coronary Artery Disease Risk Locus

Introduction

The 9p21.3 Coronary Artery Disease Risk Locus' Role in ARF regulation

At a transcriptional level, there have been many studies looking into the regulation at the *ARF* promoter. It is well known that in many different types of cancers, methylation of the *ARF* promoter occurs and it has been shown that a CpG island exists near *ARF* promoter with hypermethylation of these sites results in silencing of gene transcription (Robertson and Jones, 1998). In contrast, Sp1 can bind to these same CpG sites and likely acts in concert with E2F1 as transcriptional activators (Parisi et al., 2002). What had not been investigated was the potential regulation *ARF* by enhancer elements.

Enhancer elements are short sequences within the genome that are able to bind transcription factors and increase expression of distant target genes (reviewed in (Shlyueva et al., 2014). They accomplish this feat by looping of the DNA where they come into close proximity of their target gene promoters allowing for recruitment or increased activity of POLR2A. In the pursuit to identify potential enhancer regions, many methods have been established for their detection. For example, many enhancer regions contain histone modifications such as H3K4me3 and H3K27ac. In addition, if an enhancer is active or primed, the DNA will be in an accessible state which can be detected by DNase activity. If the DNA is inaccessible and does not show characteristic histone modifications, conservation of sequences in gene desert regions can be used as an indicator of latent enhancers.

One such potential enhancer of *ARF* expression is the 9p21.3 coronary artery disease (CAD) risk locus. This locus was first identified through a genome-wide association study (GWAS) by the Hobbs-Cohen lab (McPherson et al., 2007). They mapped an interval spanning

approximately 58 kb in which single nucleotide polymorphisms (SNPs) correlated with coronary heart disease to a high degree of statistical significance ($p<0.01$) (Fig 2.1A and B). This region is approximately 85 kb from *ARF* exon 1β is not known to encode any genes, yet in a meta-analysis of GWAS studies this region contained SNPs also associated with cancer, type 2 diabetes, and other age-related diseases (Jeck et al., 2012).

To study how this risk interval influences these diseases, the Pennachio lab created a mouse model in which the 70 kb orthologous region on mouse chromosome 4 was deleted (Fig 2.1C and D) (Visel et al., 2010). In these chr$^{\Delta 70kb/\Delta 70kb}$ mice, survival at all periods of life decreased, while weight and tumor incidence increased compared to wildtype. They next looked

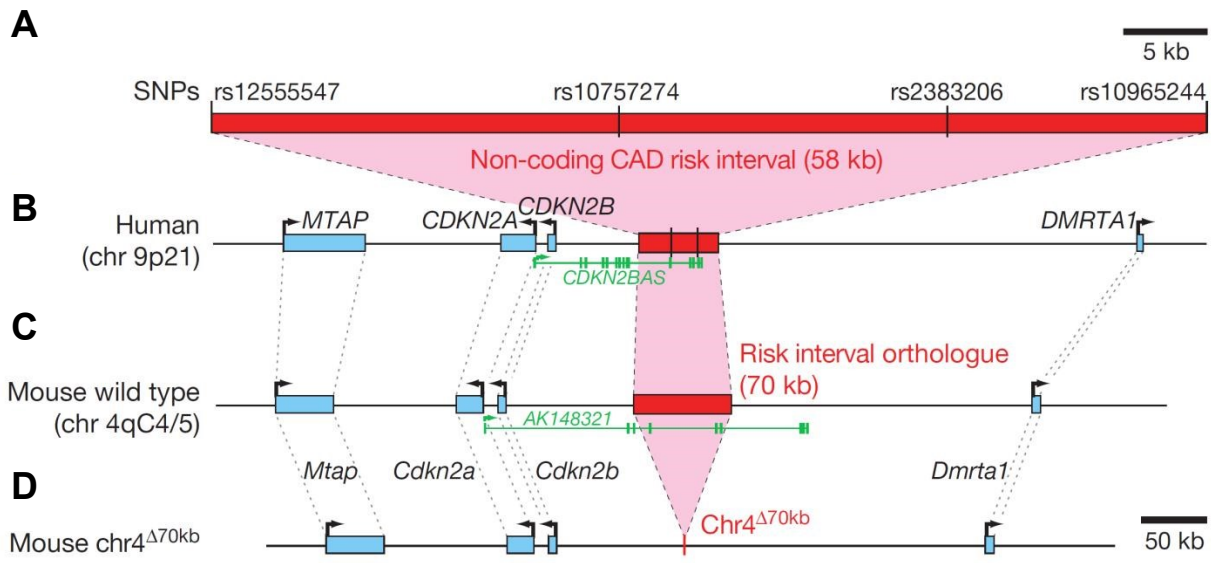

Figure 2.1: Schematic of the CAD risk interval and knockout of orthologous region in mouse. A) The 9p21.3 CAD risk interval and SNPs that are significantly linked to increase coronary artery disease risk. The risk interval is located approximately 85kb downstream of the *CDKN2A*/*ARF*/*CDKN2B* locus in humans (B) and 110kb downstream in the mouse orthologous region (C) with non-coding RNA transcripts shown in green. D) In chr4$^{\Delta 70kb}$ mice, the orthologous risk interval has undergone a homozygous deletion (modified from Visel et al., 2010).

at the expression of nearby genes in chr$^{\Delta 70kb/\Delta 70kb}$ mouse heart tissue and found that both *Cdkn2a* and *Cdkn2b* levels were nearly abolished (Fig 2.2). Interestingly, when 129sV chr$^{\Delta 70kb/\Delta 70kb}$ mice were crossed with C57BL/6 chr$^{+/+}$ and *Cdkn2b* transcript abundance was determined by strain-specific SNPs, the predominant sequence was from the C57BL/6 mouse allele. This suggested there exists an enhancer element capable of affecting the *Cdkn2a/Arf/Cdkn2b* locus.

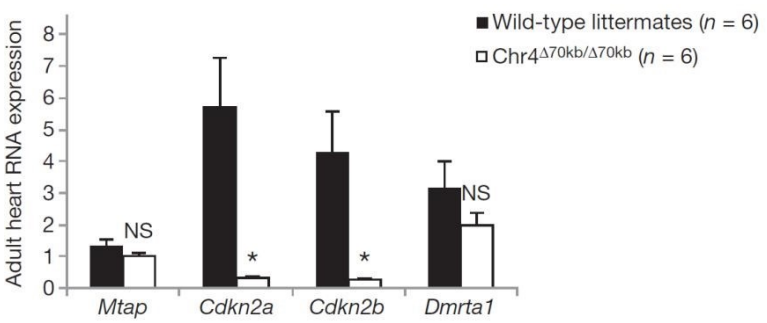

Figure 2.2: Loss of the orthologous CAD risk interval in mice results in decreased *Cdkn2a/Cdkn2b* expression. Compared to mice that have the intact orthologous 9p21.3 CAD risk locus, in the hearts of mice which harbor a homozygous deletion Cdkn2a and Cdkn2b expression is nearly abolished while the two genes flanking the locus (Mtap and Dmrta1) are unaffected (modified from Visel et al., 2010).

Based on the findings from Pennachio's group, the Skapek lab asked if deleting the 9p21.3 orthologous risk had the same effect on *Arf* expression and it's response to Tgfβ. They observed that not only did chr$^{\Delta 70kb/\Delta 70kb}$ mice display the same PHPV-like phenotype but that basal *Arf* levels in chr$^{\Delta 70kb/\Delta 70kb}$ MEFs was nearly abolished and Tgfβ lost its ability to initiate induction even though Smad2/3 was detected at the *Arf* promoter (Zheng et al., 2013). To further explore the possibility of Tgfβ-responsive, *cis*-acting regulatory elements existing in the risk locus, chr$^{\Delta 70kb/\Delta 70kb}$ mice were crossed with *Arf*$^{lacZ/lacZ}$ mice. This produced a double heterozygous knockout in which one allele contained intact *Arf* with the risk locus deleted while the other allele had exon 1β replaced by *lacZ* with the risk locus intact (Fig 2.3A). When *Arf*$^{lacZ/+}$ chr$^{+/\Delta 70kb}$ MEFs were treated with Tgfβ, they showed increased β-gal expression but no increases in *Arf* exon 1β mRNA when compared to wildtype MEFs (Fig 2.3B and C). Though basal *Arf* mRNA and protein levels were almost undetectable in chr$^{\Delta 70kb/\Delta 70kb}$ MEFs, ectopic

expression of oncogenic human H-RAS was able to increase $p19^{Arf}$ levels, albeit at lower total levels than wildtype MEFs (Fig 2.3D).

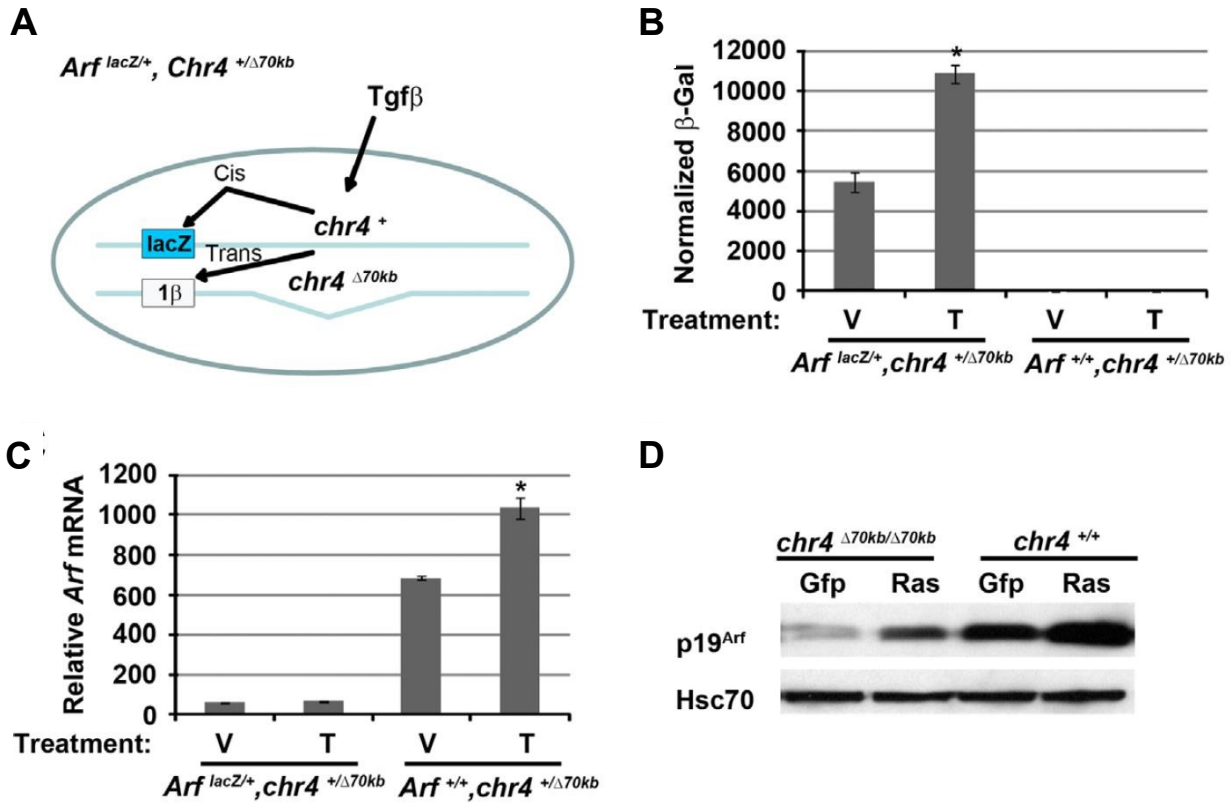

Figure 2.3: The orthologous CAD risk interval acts in *cis* of the *Arf* gene and ablates *Arf* expression in response to TgfβI but not oncogenic stimuli. (A) Diagram showing the dual hetero-transgenic mouse with the exon 1β of *Arf* replaced with *lacZ* but retaining intact orthologous CAD region on one allele, while the other allele contains wildtype *Arf* with the orthologous CAD region deleted. (B) β-gal assay showing *lacZ* is functional and expression increases in response to Tgfβ2 in dual-het MEFs. (C) In contrast, *Arf* mRNA is not induced in the same dual-het MEFs along with lower basal expression when compared to single-het $chr4^{\Delta 70kb}$ MEFs. (D) Ectopic expression of oncogenic Ras results in $p19^{Arf}$ induction, though levels are decreased in $chr4^{\Delta 70kb/\Delta 70kb}$ MEFs (modified from Zheng et al., 2013).

These data clearly demonstrated that a regulatory element existed in the orthologous 9p21.3 CAD risk locus, that it acted in *cis* to *Arf*, and that it affected the ability of Tgfβ to induce *Arf* expression. The Skapek lab had a clear interest to identify the mechanism by which this element acted upon *Arf* in response to Tgfβ. I decided to pursue this interest and took over a project from Caroline Sung, a MD/PhD student at the time, focused on detecting whether a

region of DNA within this risk locus looped around to recruit a transcriptional co-activator at the *Arf* promoter in MEFs. To do so, we chose the chromosome conformation capture (3C) technique pioneered by Job Dekker (Dekker et al., 2002).

The 3C technique is able to capture and detect when DNA regions of interest come into close proximity to one another, either at normal steady-state or in response to some stimuli, and has been used to detect distant regulatory elements. This is accomplished by choosing a restriction enzyme (RE) that cuts DNA once near the promoter of your gene of interest (GOI) and also cuts at the potential regulatory elements of interest so that the resulting fragments are between 1-10 kb, ideally in the middle of this range (Naumova et al., 2012). An anchor primer is

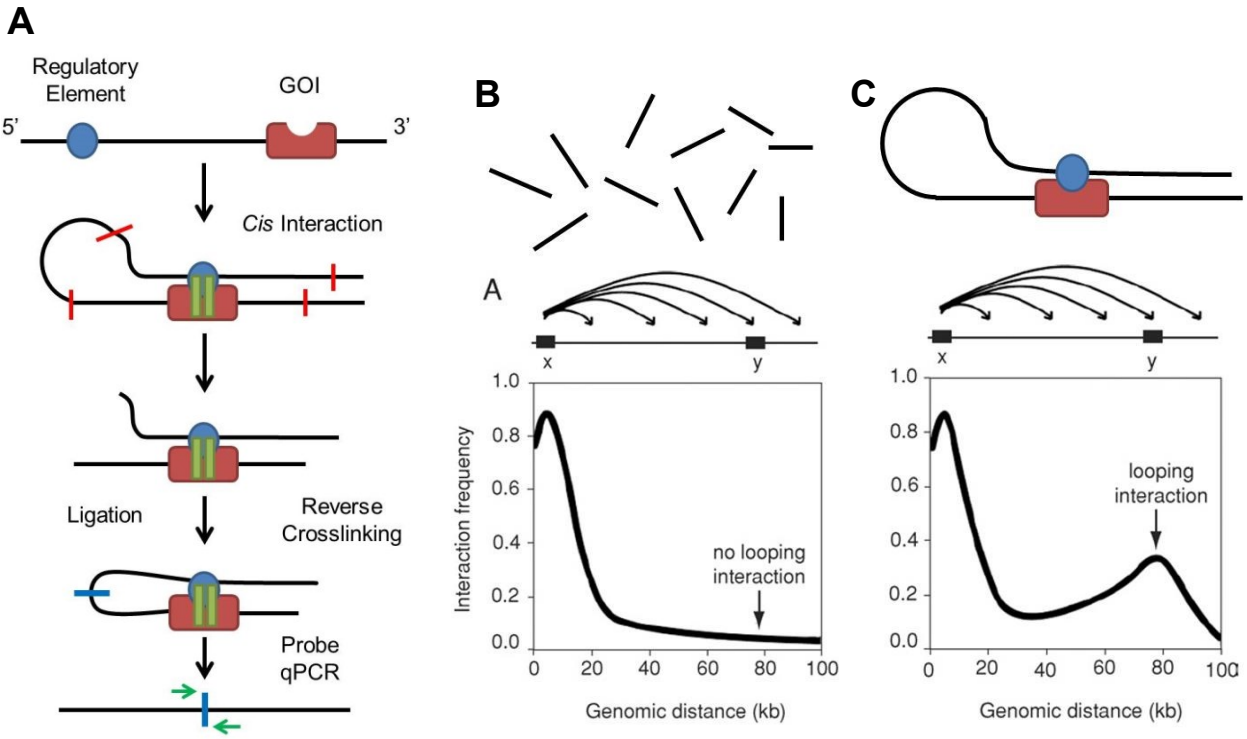

Figure 2.4: Schematic diagram of the 3C technique and expected results. A) diagram demonstrating the how 3C captures interacting regions of DNA through crosslinking, digestion, ligation, reverse crosslinking, and finally probe qPCR to detect the expected ligation product. If there is no interaction, the expected result would be decreased interaction frequency the further away the two regions are due to stoichiometry (B) while regions that do loop together will be at a higher frequency than can be attributed to randomness (C) (modified from Miele et al., 2006).

designed near the restriction site of your GOI with a TaqMan probe developed on the opposite strand to detect rare interactions. Primers at the restriction sites for the regulatory elements should be designed so that if the digested GOI and regulatory element are ligated together, elongation by PCR can take place.

After all these requirements are met, cells under the conditions chosen for the experiment are treated with formaldehyde to crosslink and capture DNA in its current conformation. From there, the DNA is digested, ligated, and reverse crosslinked. TaqMan probe real-time quantitative PCR (qPCR) is performed to detect if there is any interaction between the GOI and potential regulatory elements, and depending on the experimental setup, at what frequency this occurs.

I decided to target potential enhancer containing regions that had been identified by a previous group. This group found four conserved noncoding sequences (CNS) within the human 9p21.3 CAD risk locus (Jarinova et al., 2009). When these regions were coupled to a minimal promoter driving *luc2* expression, two CNSs demonstrated the ability to act as transcriptional enhancers. With this in mind, I proceeded to design and test a 3C protocol to detect whether chosen regions in the orthologous 9p21.3 CAD risk locus looped into close proximity of the *Arf* promoter in response to TGFβ1 in MEFs.

Methods

Plasmids and primer design

Bacterial artificial chromosomes containing minimally overlapping regions encompassing the orthologous loci for *Cdkn2a/Arf/Cdkn2b* and 9p21.3 CAD in mice were obtained from Riken Bioresource Center DNA Bank and used to validate primers used in 3C. Anchor primers were designed in the first intron of *Arf* transcriptionally before the first *BglII* restriction site. TaqMan probes were designed on the antisense strand before the first *BglII* site but after the anchor primers. Primers targeting the CNS regions were designed on the same strand as the anchor primer before the *BglII* sites within and around each CNS region. As a positive control, primers were designed at *BglII* sites within and around the *Gapdh* locus, as described in Spilianakis and Flavell (2004). For the full list of primers used, see appendix.

Cell culture

Primary MEFs were obtained from the second generation of wildtype C57BL/6 x 129/Sv mice at E13.5 and cultivated as previously described (Freeman-Anderson et al., 2009; Silva et al., 2005; Zindy et al., 2003). Early passage MEFs (less than seven passages) were used for each 3C experiment and cultured in 15 cm cell culture plates.

Chromosome conformation capture

The protocol for 3C was based upon previously established techniques by Hagege et al. (2007) with the following modifications. Briefly, *BglII* restriction enzyme was used at 2X and 5X amounts including boosts both after the overnight digestion and 2 hr after the initial boost for

some experiments. Cell density was decreased from $1.0x10^7$ to $0.5x10^7$ for the first digestion conditions test and other variations were made according to suggestions listed in by Hagege et al. (2007).

TaqMan probe real-time quantitative PCR

Purified DNA from the ligated, reversed crosslinked 3C samples were subjected to TaqMan probe qPCR with the validated 3C primers on Bio-Rad's C1000 Touch thermal cycler. KAPA's 2x probe qPCR mix at a final volume of 10 µl for each reaction in triplicate while capture was performed with Bio-Rad's CFX96. DNA concentrations were measured by nanodrop and diluted to a final concentration of 20 ng/µl, of which 1 µl (20ng) was used for each reaction. Anchor and target primers for each region of interest were added for a final concentration of 400 nM with TaqMan probe added for a final concentration of 200 nM. Optimized qPCR cycling conditions were determined to be 3 min at 95 ^oC, followed by 40 cycles of 3 s at 95 ^oC and 30 s at 58 ^oC.

Results

Ligation products from BglII digested and randomly ligated Cdkn2a/Arf/Cdkn2b and 9p21.3 CAD BACs can be detected using probe qPCR

The selection of the restriction enzyme is the first and perhaps most crucial step in the 3C process. As the experiment was a candidate approach, I considered REs that would generate low complexity and decided upon "6-cutter" enzymes that would decrease the resulting number of digest fragments. It is important for the RE to have high digest efficiency, and considering that *Arf* is a CpG island, I would need to select an enzyme able to cleave methylated DNA. Previous attempts by Caroline Sung were based on digestion with *EcoRI* and were unsuccessful due to the inability to detect any reliable signals when validating her primer set. To avoid any complications that might be contributed to *EcoRI* digestion in this setting, I opted to use *BglII*, a "6-cutter" RE that recognizes the sequence 5'-AGATCT-3' and cleaves after the first adenine nucleotide. In addition to being able to cleave methylated DNA, restriction site frequency was low at the CNS regions and *Arf* promoter, producing fragments that fell within the specified length (1-10 kb) for detection of crosslinked DNA fragments (Fig 2.5).

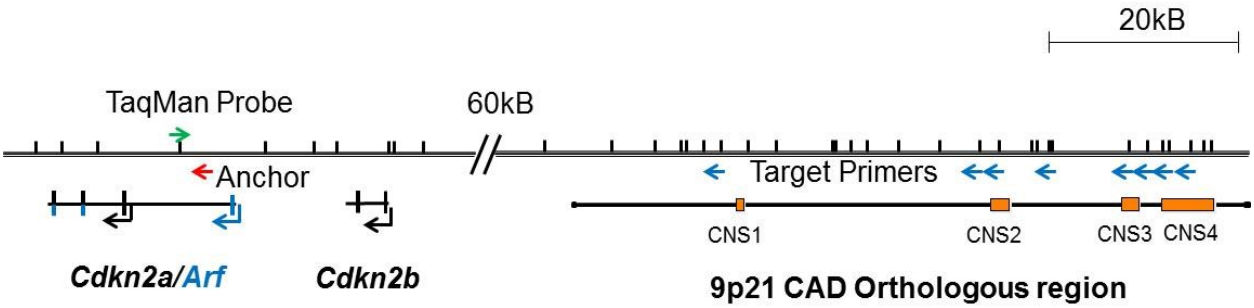

Figure 2.5: Schematic representation of the primer design for the 3C experiment. Anchor primers (red) were created before the first transcriptionally downstream *BglII* (black notches) in the first intron of *Arf* (light blue) with the TaqMan probe directly before the anchor primer. For the CNS regions (orange), target primers (blue) were created at the *BglII* sites in and immediately around each region.

With *BglII* as the chosen RE, I designed primers at the restriction sites near or within the regions of interest. An important consideration during primer design was to ensure that primers were both on the same strand and priming in the same direction (Fig 2.5). This is due to the fact that this is sticky-end ligation and one strand will be in the opposite orientation relative to its position in the chromosome. The anchor primer determines what direction the region of interest primers would face, and due to the highly repetitive, CpG rich DNA transcriptionally upstream of the *Arf* promoter, I chose to locate the anchor primer downstream (Fig 2.5). Based upon two separate anchor primers at this region, I designed two sets of CNS primers, each with 1-2 separate primers for each CNS in case of poor detection from any one primer pair.

Each primer pair was designed using a template from the GRCm38/mm10 mouse genome in which I performed ligation *in silico* based upon *BglII* digest. From each ligation product, a 600 bp segment with the ligation site in the center was copied into the Primer3Plus primer design program. The ligation site was chosen as a target with the anchor primer used as input for the left primer and conditions where adjusted for probe qPCR. This program was also used to design the TaqMan probe between the anchor and its restriction site on the opposite strand The resulting list of primers were analyzed both by Primer-BLAST to ensure specificity and IDT's OlgioAnalyzer 3.1 tool to check for secondary structures. Using these analyses, the highest specificity primers were chosen.

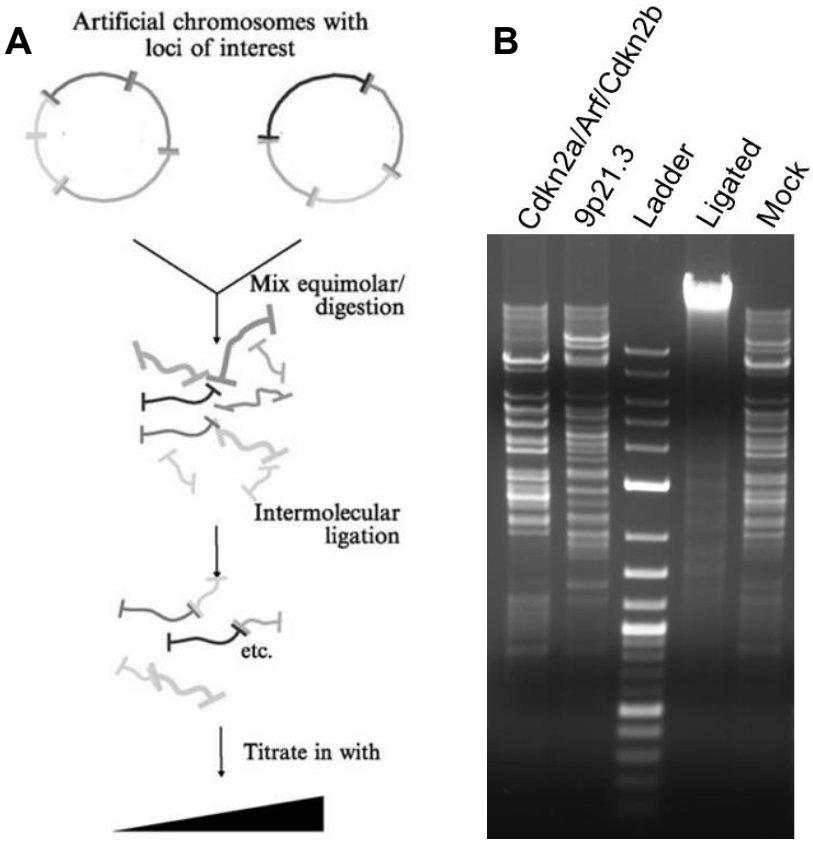

Figure 2.6: Primer validation of 3C using BACs. A) Schematic of primer validation using two minimally overlapping BACs digested and ligated in equimolar concentrations (modified from Splinter et al., 2004). B) Ethidium bromide stained agarose gel showing individual digestion of both BACs separately next to an equimolar mixture of each ligated and mock ligated.

To validate each primer pair, I utilized two BAC constructs with minimally overlapping regions encompassing the *Cdkn2a/Arf/Cdkn2b* and orthologous 9p21.3 CAD risk locus. Following conventional 3C protocols, the two BACs were mixed together in equimolar concentrations, digested with *BglII*, and randomly ligated together (Fig 2.6 A). When the ligated mixture was run on an ethidium bromide agarose gel, one dominant band appeared. As expected, both BACs individually digested and a combined mock ligation showed bands of predicated molecular weight for *BglII* digest (Fig 2.6 B). The primers were used in probe qPCR with two different concentrations of the ligated BACs as a template. For a primer pair to be validated and consider for experimental use, the specific PCR product must be the only band present with PCR efficiency between 90-110% (Fig. 2.7 A-C). I validated a full set of primers covering each CNS region using these criteria.

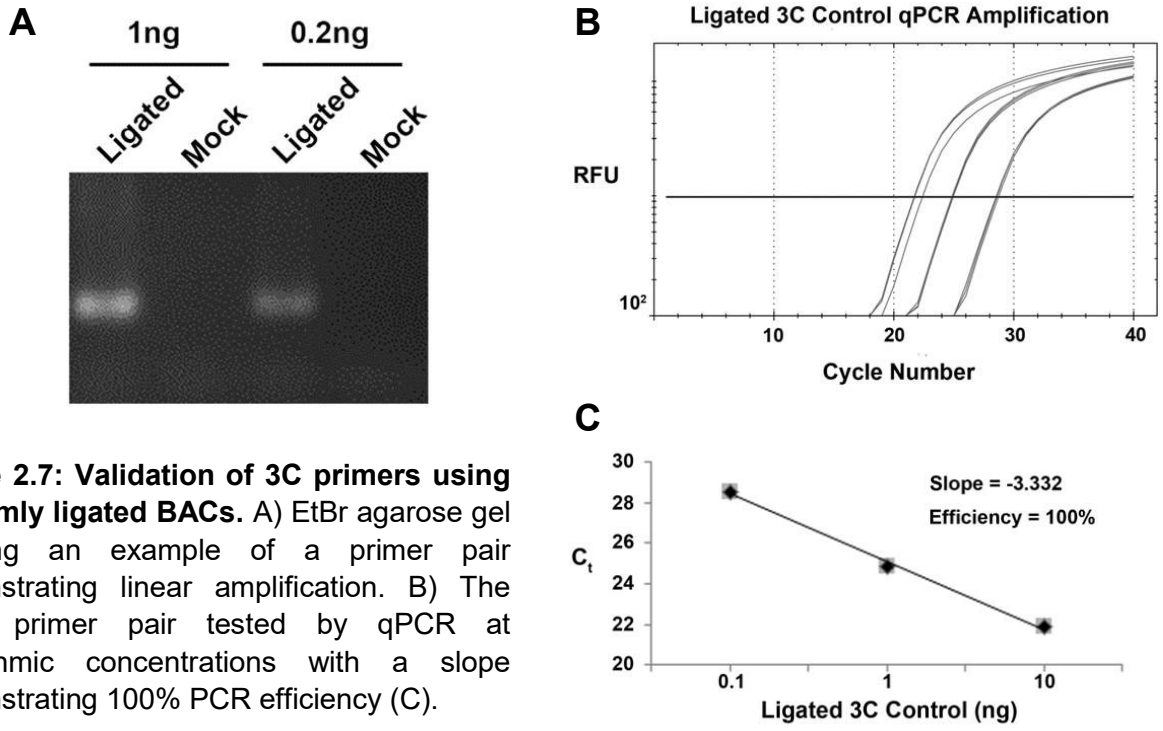

Figure 2.7: Validation of 3C primers using randomly ligated BACs. A) EtBr agarose gel showing an example of a primer pair demonstrating linear amplification. B) The same primer pair tested by qPCR at logarithmic concentrations with a slope demonstrating 100% PCR efficiency (C).

Optimization of 3C results in high BglII digest efficiencies but fails to detect interactions in MEFs

The nucleus is filled with molecular machinery in addition to nucleic acids, and this can lead to difficulty in detecting looping interactions with crosslinking difficult. To increase the ability to detect interactions that could occur at low frequency, high RE digestion efficiency is needed at each site being interrogated. In the literature, many groups have developed and refined the 3C technique, so I based my initial experimental protocol on a detailed methods paper from the Forné lab (Hagege et al., 2007). For a positive control, I looked to another group that had used the *Gapdh* locus with the *BglII* enzyme in a 3C experiment (Spilianakis and Flavell, 2004). Focusing on the first two sets of primers used, I adapted this control to my experiment (Fig 2.8). To identify the optimal conditions needed to achieve high *BglII* digestion efficiency, I performed each experiment using genomic DNA from wildtype MEFs with one procedural variation up until the addition of ligase, in which I mock treated the 3C sample to reflect a true experimental run.

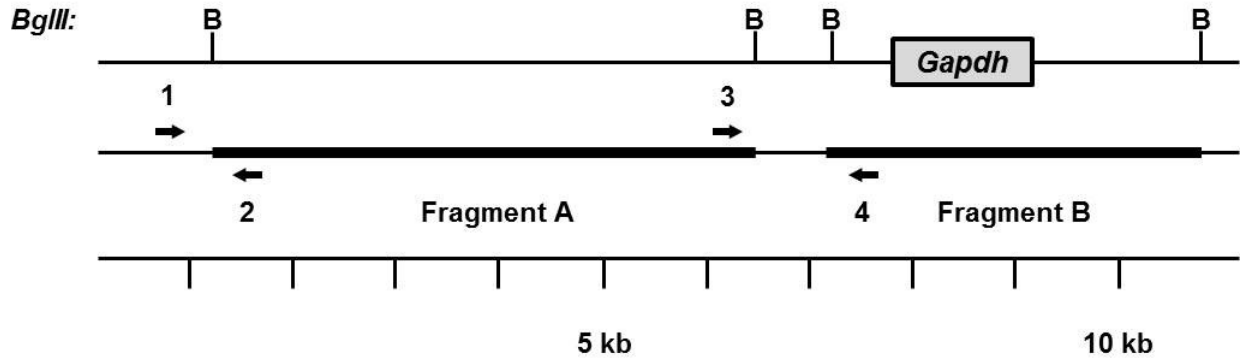

Figure 2.8: Diagram of 3C control centered near the *Gapdh* locus. In mice, *BglII* sites are located at 4 different regions near and around the *Gapdh* locus resulting in two different fragments. Due the proximity of the sites and fragments to one another, a detectable signal can be assayed due to proximity. For this 3c experiment, primers 1=4 were chosen (modified from Spilianakis and Flavell, 2004).

I first chose to test a set of RE digest conditions based on cell confluency at harvest, the initial dose of RE used for digestion, and a "boost" dose of RE for 2 hr after the initial overnight digest (Fig 2.9). The baseline condition was adhering strictly to the Forné lab's protocol with the use of a detergent-based lysis buffer. *BglII* digest of the orthologous 9p21.3 CAD BAC was used as a positive control. Cell density had little effect on *BglII* digestion, while increasing the initial RE dose showed incremental improvements with increased concentration at most sites. The overnight boost of RE was as efficient as a 5x dose, which when taken together with the 7 hr activity half-life of *BglII*, is an expected outcome. Though some sites were able to reach efficiency higher than 60%, the *Arf* anchor site did not, which meant further optimization was needed. While not shown here, *BglII* digest efficiencies for the *Gapdh* locus were near or above 60% for boost and 5x RE dose conditions.

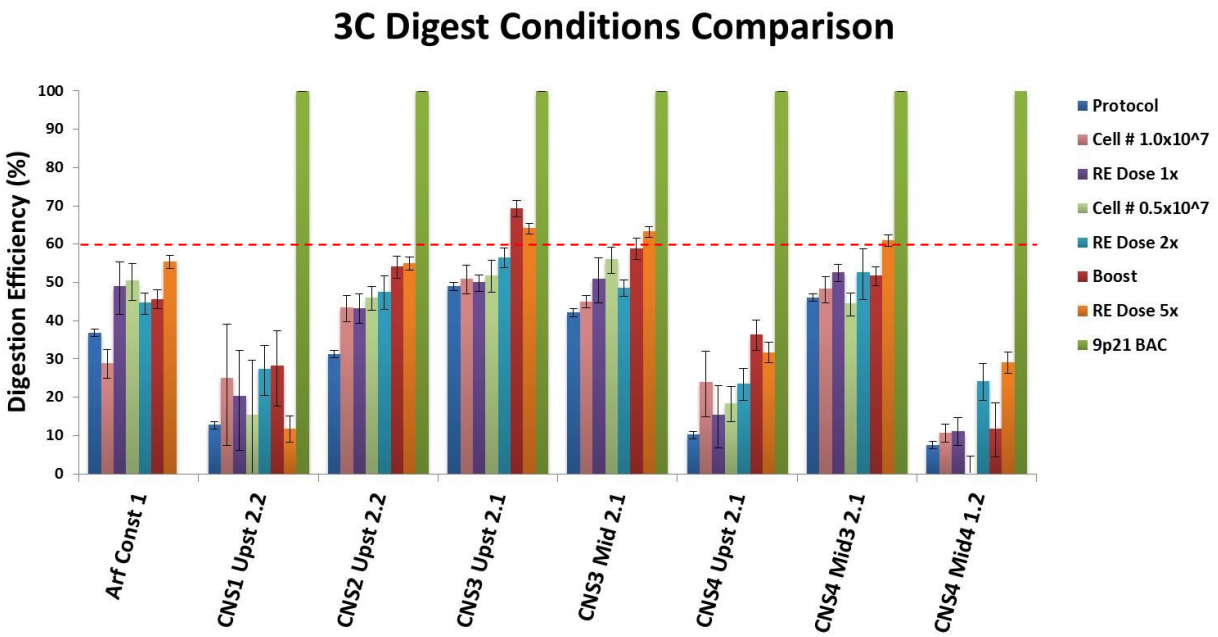

Figure 2.9: Graph of digest optimization. Chart showing the mouse genomic DNA digest efficiencies of multiple different conditions leading up to and immediately after addition of restriction enzyme *BglII* as measured by qPCR in comparison to non-digested sample with the 9p21.3 CAD orthologous region BAC as control for the CNS regions. Digest efficiencies were highest for boost (red bar) and 5X RE (orange bar) but did not meet the 60% threshold for many sites (red dotted line).

I decided that further improvement was needed and proceeded to test a second round of conditions, building upon my results and using 5x RE as the baseline for this test. The initial concentration of formaldehyde, which is known to influence RE digestion, along with changes to the "boost" RE dose, lysis buffer, and physical membrane disruption were made (Fig 2.10). Physical disruption of the cellular membrane seemed to have little effect, while lack of detergent in the lysis buffer severely decreased efficiency at many sites. Decreasing formaldehyde and adding a second "boost" greatly increased *BglII* digestion at many sites, including *Arf* at 60% efficiency. With the optimal conditions for, and leading up to, the RE digestion established, I proceeded to carry out the full experimental method comparing MEFs with or without incubation of TGFβ1.

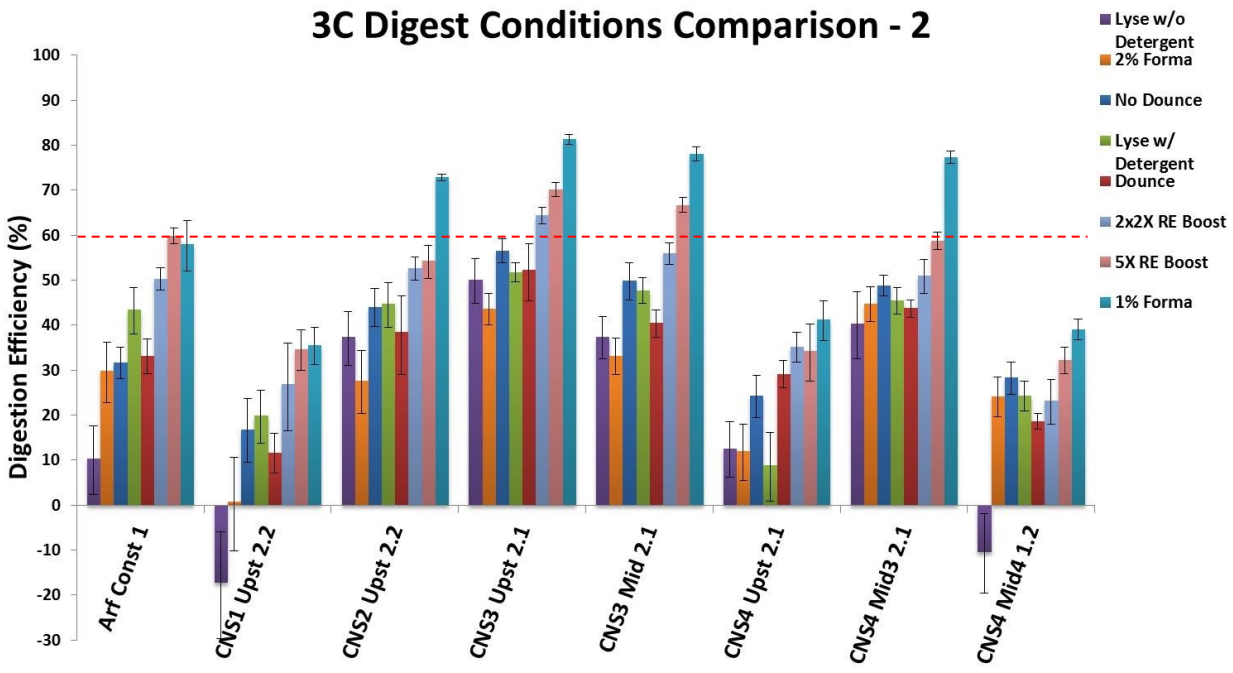

Figure 2.10: Graph of 2nd digest condition optimization. Chart showing the second set of conditions to optimize digestion efficiency under the same experimental setup and analysis as the previous test. For these tests, crosslinking with 1% formaldehyde (light blue bar) yielded the highest digest efficiency. The 5X initial RE dose and boost (pink bar) was able to achieve 60% (red dotted line) at four different *BglII* sites followed closely by a 2X RE dose with two additions of 2X RE, one after the overnight incubation and another two hours later.

Wildtype MEFs treated with either vehicle or TGFβ1 were processed following the optimized 3C protocol. Digest efficiencies for nearly all CNS regions of interest were within acceptable parameters, though the *Arf* anchor site had a large amount of variation in the non-digested samples making interpretation of digest efficiency for this region difficult (Fig 2.11A). Despite the high digestion efficiencies within the regions of interest, a reliably detectable signal was not obtained using qPCR (Fig 2.11B). Furthermore, though previously the digest efficiencies of the Gapdh control regions were at or above 60%, for this experiment they considerably below this cutoff value (Fig 2.11A).

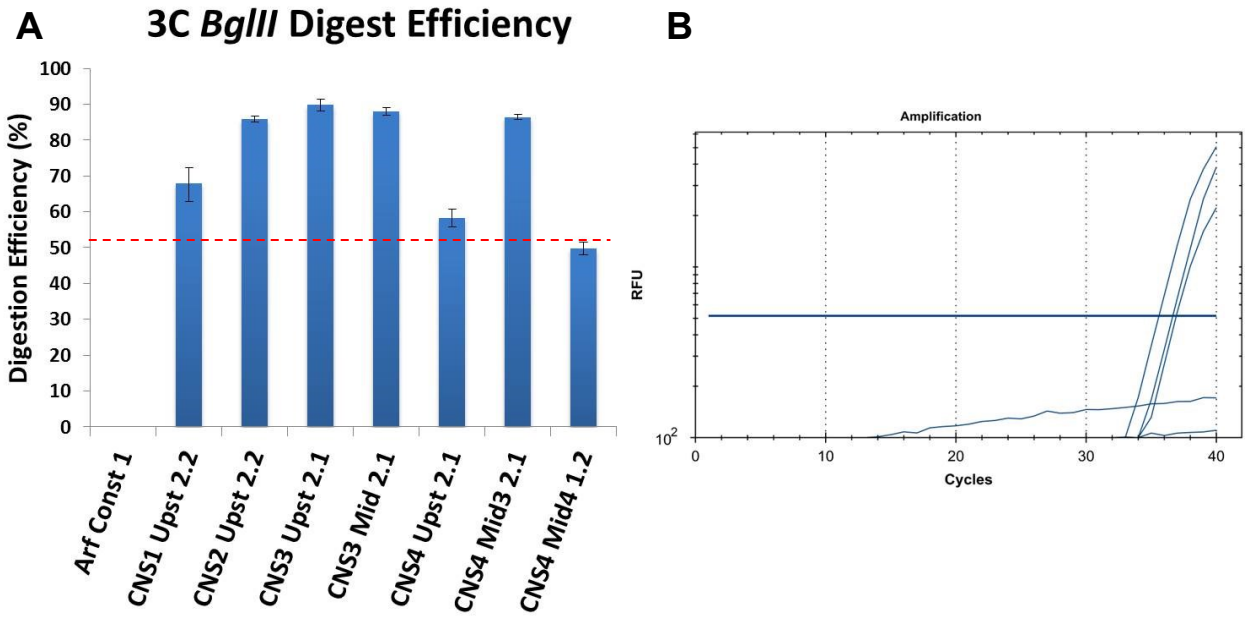

Figure 2.11: Full 3C experiment with optimized *BglII* digestion conditions fail to yield reliable signal. A) Digestion efficiencies of MEF genomic DNA with optimized digestion conditions consisting of 1% formaldehyde and 5X RE with an additional 5X boost after overnight digestion and another 5X boost two hours after. The *Arf* constant primer is not included due to technical errors during qPCR. B) Amplification curves from qPCR showing that no interactions could be detected between any of the sites targeted and the *Arf* promoter. Included in this is the Gapdh control regions assayed.

Concluding Remarks

Utilizing previous groups' work using the 3C method, I was able to develop an optimized protocol for the restriction enzyme *BglII*. Interestingly, upon analysis of *BglII* digestion efficiencies among the CNS regions of interest, a pattern emerged indicating that some sites were more open than others. Treatment and sensitivity to DNAse is a common technique used to assay whether regions of DNA are accessible to transcriptional machinery. Sites such as CNS 3 displayed a consistently high level of digestion, demonstrating that the chromatin in this region is open and accessible. This could be considered evidence that some regulatory element exists within this region.

The difficulty in obtaining an interpretable signal from the final 3C assay could be due to many reasons, including the inherent difficulty in detecting interaction of two DNA elements among approximately three billion DNA basepairs. As mentioned previously, *Arf* is a CpG island meaning there is a high amount of repetition in this area. This presents additional obstacles when designing primers around this region, and I encountered this when I was only able to prime one *BglII* site next to *Arf* as the other site yielded primers that had a high amount of mispriming.

Though my attempt at directly identifying suspected regulatory elements failed, the evidence that these exist within the orthologous 9p21.3 CAD risk locus is still strong. Moving forward, a less biased approach could provide a more accurate view of where these enhancer elements reside. For example, using RNA-seq to uncover what histone modifications exist in the risk locus, including those indicative of enhancer elements such as H3K4me3 and H3K27ac, would be a wise experimental approach.

CHAPTER 3:

Absence of TGFβ-Dependent Induction of *ARF* in Select Lung Cancer Cell Lines

Introduction

Lung cancer is and will continue to be one of the leaders in new cancer cases and deaths in the US. It is estimated that in 2016, over 200,000 new cases of lung cancer will be diagnosed along with over 150,000 deaths from this disease. Those who are diagnosed face very poor outcomes as lung cancer has one of the lowest 5-year survival rates at 18%. There are three main types of lung cancer, though non-small cell lung cancer (NSCLC) is the highest occurring with approximately 85% of cases belonging to this group.

The role of *ARF* in NSCLC has remained unclear as different groups have presented conflicting results. While some groups have shown there to be mutually exclusive inactivation of *ARF* with p53 or overexpression of MDM2, others have shown that these events do co-occur (Mori et al., 2004; Park et al., 2003; Sanchez-Cespedes et al., 1999; Wang et al., 2005). This could be reconciled by the understanding that *ARF* can act as a tumor suppressor in p53-dependent and independent manners. Unfortunately, a comprehensive study of NSCLC examining all the possible modes of inactivation for *ARF* specifically and not in concert with $p16^{INK4A}$ has not been undertaken, leaving open the possibility that *ARF* plays an important role in oncogenesis and/or disease progression.

For TGFβ, it has been well established that it switches from a tumor suppressor to an oncogene in lung cancer. Early in the disease, the growth suppressive and apoptotic effects of TGFβ are still intact leading to very low levels in lung tumor cells and the surrounding environment (Roberts and Wakefield, 2003). At later stages of lung cancer progression, upregulation of TGFβ with concurrent alterations to the signaling pathway correlates to poor prognoses and increase in malignancy (Fig 3.1) (Levy and Hill, 2006). For NSCLC, this is due in part to the overexpression of inhibitory SMAD6 in tumor cells thus disabling the growth

suppressive effects of TGFβ as well affecting the microenvironment surrounding the tumor by promoting angiogenesis and loosening the junctions between endothelial cells (Lebrun, 2012).

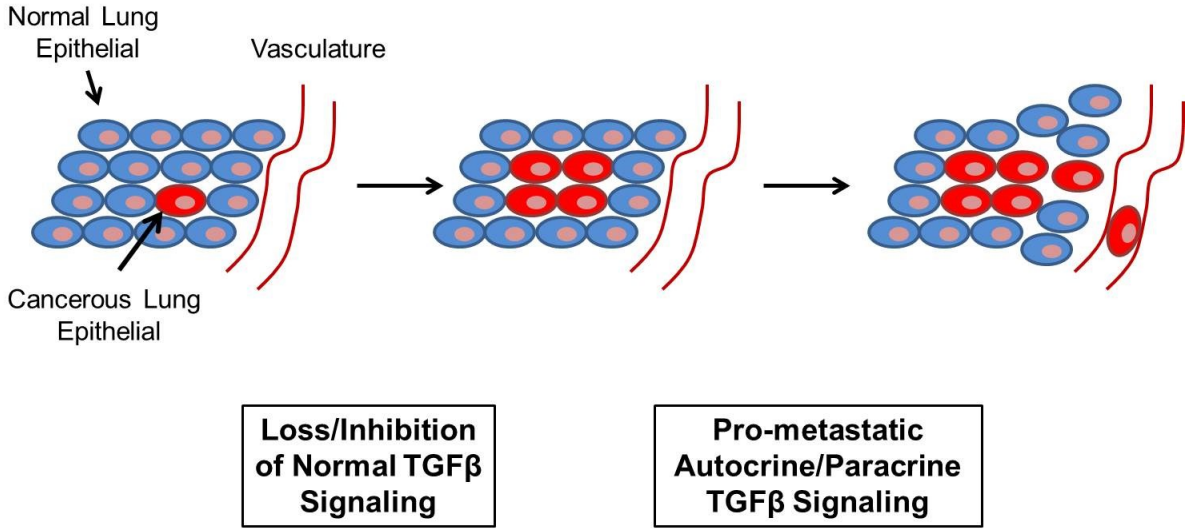

Figure 3.1: Representation of the influence of TGFβ in lung cancer progression. At the beginning stages, lung cancer cells can still be influenced certain growth suppressive signals including TGFβ. As the disease progresses and mutations are accumulated, many of these growth suppressive pathways are bypassed, by inhibitory signals and/or mutation or deletion of key components, allowing for the further progression of lung cancer. In the case of TGFβ, sufficient suppression of tumor suppressive effects can lead to it promoting cell motility and metastasis, thereby switching its role to an oncogene.

Due to the importance of TGFβ in NSCLC progression, I asked the question of whether cells lines derived from this disease would respond to TGFβ by inducing *ARF*, similar to what has been observed in HeLa cells. The Skapek lab has previously shown that ARF expression is induced in response to TGFβ and I have reproduced these results. What is unknown are what components in the human TGFβ pathway are required for *ARF* response and whether this phenomenon occurs in other cancer cells. In mice, we know that SMAD2 and SMAD3 play a role in induction as well as p38, a component of the non-canonical pathway. This provided me the opportunity to ask if the same proteins were involved in TGFβ-dependent *ARF* induction in HeLa cells and how these findings translated to a panel of NSCLC cells.

Potential for TGFβ dependent induction of ARF as a possible contributor of oncogenesis

The finding that *ARF* can be induced in response to TGFβ, at least in HeLa cells, opens questions as to how this pathway might be regulated in NSCLC and what can be learned and utilized from this information towards management of the disease. For example, if the TGFβ/$p14^{ARF}$ pathway is intact in the early stages of NSCLC along with wildtype p53, TGFβ could potentially be used as an early stage treatment measure at a stage in which loss of normal TGFβ signaling has not occurred. If the pathway is disrupted, then by identifying aberrations in the signaling cascade and subsequently restoring functionality to those components could result in reactivation of *ARF* through TGFβ. I set out to address these possibilities by compiling a small panel of NSCLC cell lines with wildtype *ARF* and *p53*. Using this cell line panel, I asked if TGFβ could induce *ARF* in these lines and if not, could restoration of important mediators that the Skapek lab has identify restore this induction.

Methods

Cell lines and cell culture

Lung cancer cell line stocks HBEC3kt, HBEC30kt, H290, H1666, HCC1833, H1944, H2172, H2347, and H2405 were obtained through the generosity of the Minna lab. All cancer cell lines including HeLa were cultured in RPMI supplemented with 10% fetal bovine serum and with penicillin and streptomycin. HBEC cell lines were cultured with keratinocyte serum free medium supplemented with bovine pituitary extract and EGF. All cell lines were incubated at 37 ^{o}C with 5.0% CO_2.

Reverse transcriptase real-time quantitative PCR

Total RNA was extracted from cells on-plate using TRIzol at approximately 80-90% confluency and treated with either 5 ng/ml of TGFβ-I or vehicle (10μM HCl, 25μg/mL BSA) for 1, 24, or 48 hr. cDNA was created from the extracted RNA according to the manufacturer's guidelines (Invitrogen SuperScript III). Purified cDNA samples were subjected to probe qPCR with the validated primers on Bio-Rad's C1000 Touch thermal cycler. KAPA's 2X SYBR Green qPCR mix at a final volume of 10 μl for each reaction in triplicate while capture was performed with Bio-Rad's CFX96. Primers for each region of interest were added for a final concentration of 200 nM with 1 μl of cDNA. Optimized qPCR cycling conditions were determined to be 3 min at 95 ^{o}C, followed by 40 cycles of 3 s at 95 ^{o}C and 30 s at 62 ^{o}C. For primer list, see appendix.

Western blotting

Total protein was extracted from cells treated either with TGFβ-I or vehicle (as described previously). Briefly, cells were washed twice with 4 ºC, 1X PBS before lysis with 1X Laemmli buffer on-plate and scraped into 1.5 ml microcentrifuge tubes. Lysates were sonicated for 2 min at high power and protein concentrations were measured using the BCA assay. Protein gels were made at a concentration of 12% polyacrylamide and loaded with 25-30 µg of protein mixed with 1X Laemmili buffer to 40 µl. Gels were ran at 85V for 30 min, then at 150V for approximately 1.5 hr in buffer containing: 49.5mM Tris-base, 38.4mM glycine, 7mM (0.2%) SDS, at pH 8.3. For wet protein transfer, PVDF membranes were used with 20% MeOH in buffer containing: 40mM Tris-base, 30.4mM glycine, 5.6mM (0.16%) SDS, at pH 8.3. Blocking conditions were optimized for each antibody starting with an initial membrane block of 1:1 PBS to PBS-based Odyssey blocking buffer for $p14^{ARF}$ detection and 1:1 TBS to TBS-based Odyssey blocking buffer for all other protein detections. Primary antibody incubation was performed overnight at 4ºC in a similar incubation solution as the membrane block but with the addition of 0.1% Tween 20. Membranes were washed 6 times for 5 min each with either PBST or TBST. Secondary antibody incubation was performed with Odyssey infrared antibodies in a solution of identical composition as the primary antibody incubation solution. Membranes were washed as before and western blots were scanned using a LI-COR Odyssey infrared western imager.

Transient transfection

Transfections were carried out with FuGENE 6 according to the manufacture's guidelines (Promega). The amount of mock or MKK3b plasmid DNA used for each transfection was 3.6 µg while the FuGENE(µl):DNA(µg) ratio was 5:1 for HeLa, HCC1833, and H2172, 3 for HBEC3kt and HBEC30kt, and 2.5 for H2347. Transfection efficiencies were confirmed by co-transfection of 0.4 µg of an eGFP plasmid reporter and qualitative analysis using fluorescence microscopy.

Results

Selecting NSCLC cell lines that contain wildtype ARF

I started by looking for NSCLC cell lines that contained wildtype *ARF*, *CDKN2A*, and since I also wanted to observe what the functional outcome of TGFβ-induced *ARF* would have, wildtype p53. With the assistance and graciousness of Dr. John Minna and his lab, I was able to comb through their data characterizing several lung cancer cell lines to identify lines with the desired genotypes. Cell line data included copy number variation, mutation and methylation status, and as shown in the heat map, mRNA expression (Fig. 3.1). As a comparison to the cancer cells, I also chose two immortalized human bronchial epithelial cells (HBECs).

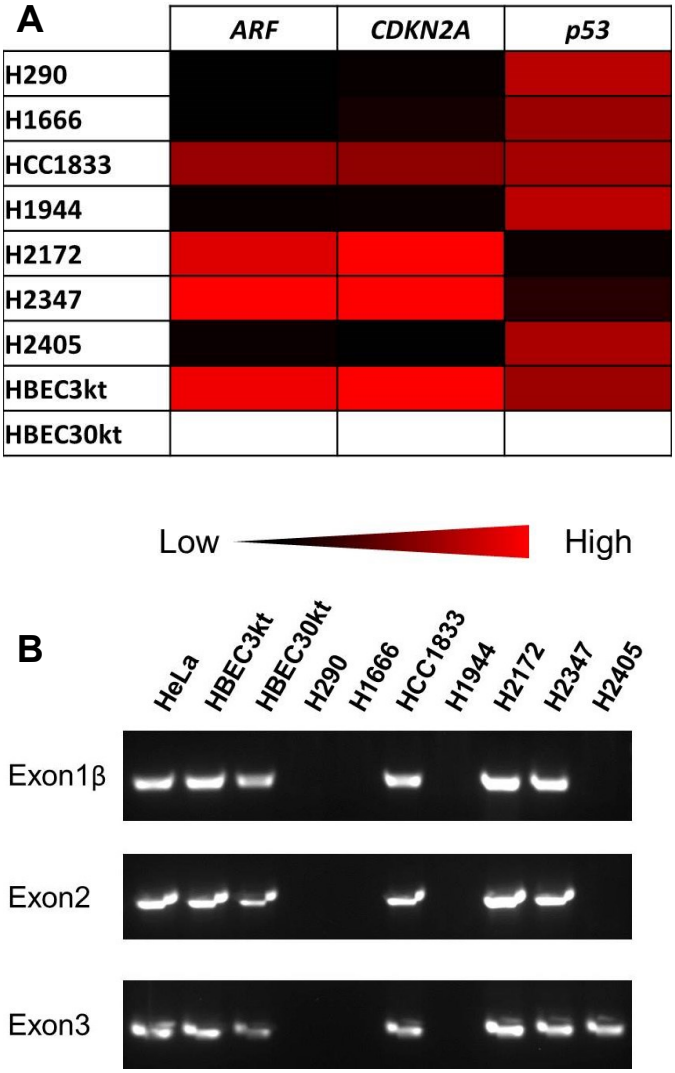

Figure 3.2: Presence of *ARF* exon 1β, exon 2, and exon 3 in lung cancer cell line panel. A) RNA-Seq data from the Minna showing expression of *ARF*, *CDKN2A*, and *p53*. B) EtBr agarose gel for confirmation of each exon in *ARF* being present and intact by PCR.

To confirm the integrity of *ARF*, I used PCR with primers for exon 1β, exon 2, and exon 3 on DNA from each of the cells lines with HeLa as a control. Surprisingly, four cell lines appeared to have deletions of some or all exons. In H290, H1666, and H1944 there was no detection of

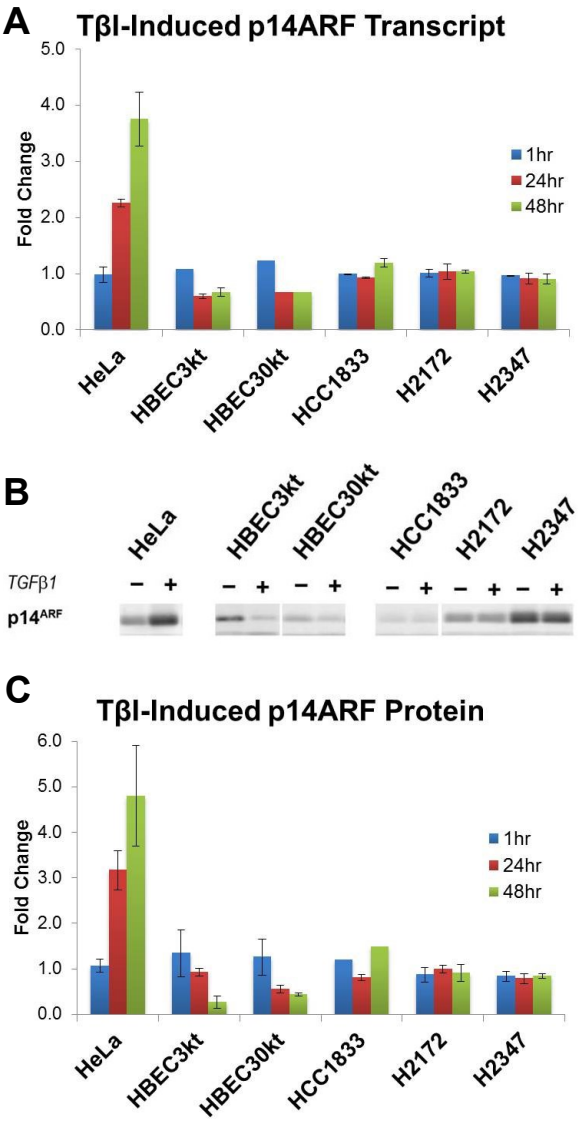

Figure 3.3: Lung cancer cell line panel fails to shown *ARF* induction in response to TGFβI. A) Induction of *ARF* in response to TGFβ1 normalized to *GAPDH* as compared to cells treated with vehicle, measured by RT-qPCR. Both conditions are first normalized to *GAPDH* and each timepoint is from three biological replicates. B) TGFβ1-induced $p14^{ARF}$ compared to vehicle treated cells as measured by western blotting. Both conditions are first normalized to HSC70 and are the cumulative of three biological replicates. C) A representative western blot showing $p14^{ARF}$ induction in response to TGFβ1.

any exons while H2405 only appeared to contain exon 3 (Fig 3.2). I removed these cells from further analysis and continued forward.

NSCLC and HBEC cell lines do not induce ARF in response to TGFβ1

To identify if any of the selected cell lines induced *ARF* in response to TGFβ1, I looked at both mature mRNA and protein expression at 1, 24, and 48 hr time points after TGFβ1 addition (Fig 3.3). Using RT-qPCR to assay changes in mature *ARF* transcript, only HeLa show increased expression in response to TGFβ1 incubation starting at 24 hr with no other cell lines showing *ARF* induction (Fig 3.3B). These results positively correlated with protein levels in all cell lines, including HeLa, when $p14^{ARF}$ expression was measured by western blotting (Fig 3.3A and B). Interestingly, HBECs showed suppression of *ARF* in response to TGFβ1 at 24 and 48 hr timepoints as observed by downregulation of *ARF* transcript and protein.

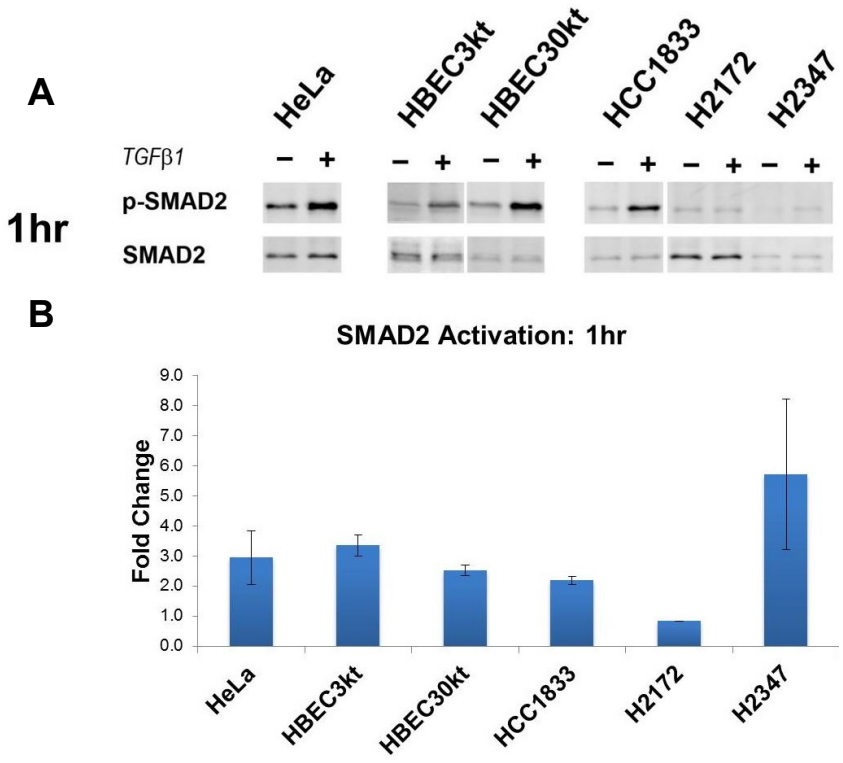

Figure 3.4: SMAD2 phosphorylation in response to TGFβ1. A) Representative western blot showing total and phosphorylated SMAD2 in response to TGFβ1 at 1 hr. B) Chart showing quantification of SMAD2 phosphorylation in TGFβ1 as compared to vehicle treated cells. Data consists of three biological replicate western blots with each condition normalized to HSC70.

NSCLC lines have defects in the TGFβ signaling components required for induction of ARF when compared to HeLa

To identify whether direct downstream components within the TGFβ signaling pathway were intact in the cell line panel, I probed for phosphorylation of SMAD2 and p38 in response to TGFβ1 as the Skapek lab had previously shown these to be important mediators of *ARF* induction. Using Odyssey infrared western blotting techniques, I asked whether SMAD2 phosphorylation levels increased after 1 hr of treatment with TGFβ1. The only cell line that failed to activate SMAD2 in response to TGFβ1 was H2172 (Fig 3.4). This provided evidence that for H2172, a dysregulation of the canonical TGFβ signaling pathway was a contributing factor to the lack of induction of *ARF* in response to TGFβ.

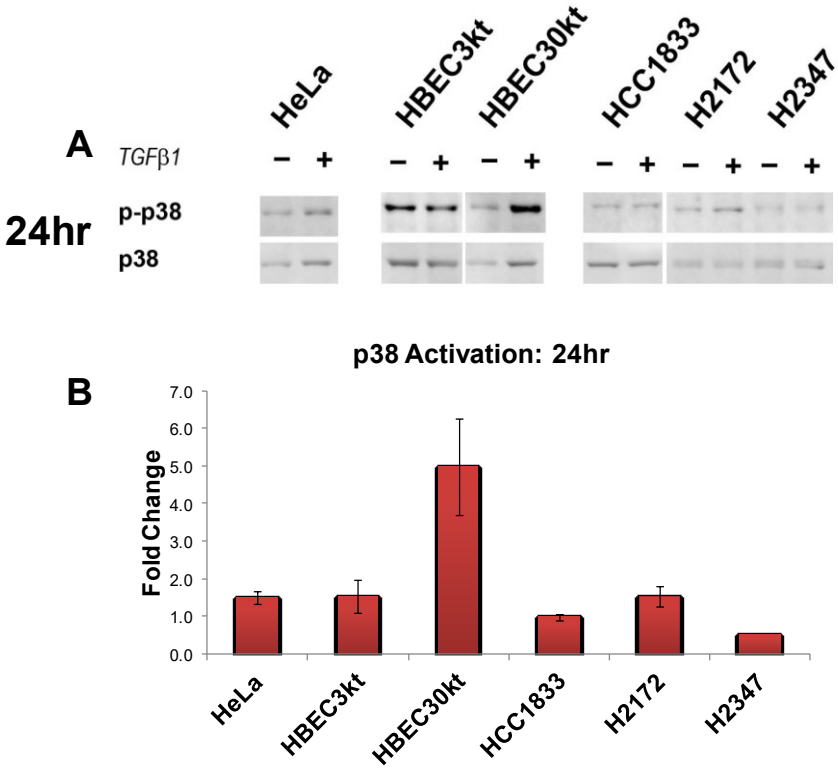

Figure 3.5: p38 phosphorylation in response to TGFβ1. A) Representative western blot showing total and phosphorylated p38 in response to TGFβ1 at 24 hr. B) Chart showing quantification of p38 phosphorylation in TGFβ1 as compared to vehicle treated cells. Data consists of three biological replicate western blots with each condition normalized to HSC70.

I used the same technique to look at p38 activation in response to TGFβ1 at 24 hr in the cell line panel (Fig 3.5). While HeLa showed a modest increase in p38 phosphorylation, there was supporting evidence from Dr. Yanbin Zheng, another member of the Skapek lab, that this was an expected observation and furthermore, when p38 activation was blocked with a small molecule inhibitor, *ARF* induction decreases significantly (data not shown). While HBECs showed an increase in p38 phoshporylation, this increase was not observed in HCC1833 and H2347. The H2172 cell line showed significant increase in p38 phoshporylation, but this cell line also lacked SMAD2 activation. These results provided evidence that the inability of TGFβ1 to induce *ARF* in these lines is due to lack of activation for components in the TGFβ pathway that were previously identified as important mediators of *ARF* induction.

With these data from activation and induction of SMAD2, p38, and *ARF* in response to incubation with TGFβ1 for 1, 24, and 48 hr timepoints in the cell line panel, a pattern emerged for the kinetics of the canonical and non-canonical components of TGFβ-dependent *ARF*

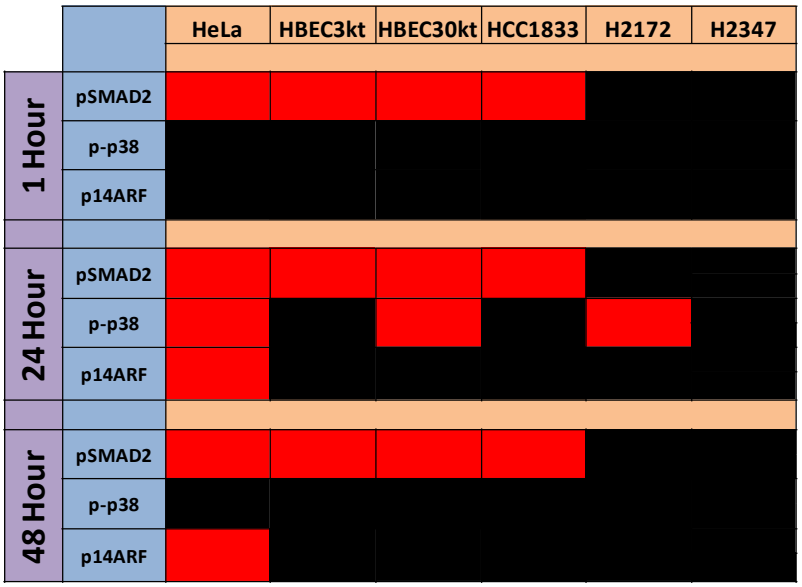

Table 3.1: Increase in pSMAD2, p-p38, and $p14^{ARF}$ at different timepoints in the cell line panel. Table showing at least 1.5 fold increases (red) in pSMAD2, p-p38, or $p14^{ARF}$ as measured by the quantification of three separate Odyssey infrared western blots. For a cell line to be considered to have an increase, it must be one standard deviation above the 1.5 threshold.

Induction	Fold Increase ≥1.5
No Induction	Fold Increase <1.5

induction (Table 3.1). For HeLa, SMAD2 is activated after incubation with TGFβ1 for 1 hr and maintains this activation while p38 only shows increase phosphorylation at the 24 hr period. In response to these signals, *ARF* expression increases at the mRNA and protein levels starting at 24 hr. These data provide a map for the signal transduction response of the TGFβ-dependent induction of *ARF* and can be used in conjunction with other data to identify irregularities in the pathway.

Forced activation of p38 does not restore nor result in increased ARF expression with or without TGFβ1 treatment

With the understanding that p38 activation is an important component of TGFβ-dependent *ARF* induction, I asked whether forcing p38 phosphorylation could restore *ARF* in non-activating cell lines and if increasing activation in HeLa resulted in increased $p14^{ARF}$ levels. To accomplish this, I transiently transfected cells with a vector containing an HA-tagged, constitutively active mutant of MKK3b (henceforth referred to as MKK3bEE), a protein that directly phosphorylates p38 in the non-canonical TGFβ signaling pathway (Fig 3.6).

In all transfected cell lines, MKK3bEE expression was confirmed as observed by blotting for the HA-tag (Fig 3.7A, H2172 not shown). In addition, when comparing changes in response to TGFβ1 versus vehicle treatment between mock and MKK3bEE transfected cell lines, no significant increase of $p14^{ARF}$ was detected in spite of basal levels of phosphorylated p38 increasing in most cell lines (Fig 3.7B, data not shown). For HeLa, there is trend of increased $p14^{ARF}$ levels in TGFβ1 treated, MKK3bEE transfected cells with two of three experiments showing higher induction, though these data seem dependent on the fact that in vehicle treated, MKK3bEE cells $p14^{ARF}$ levels are at half the amount observed for the mock control. Taken together, these data demonstrate that forced activation of p38 does not result in increased expression of $p14^{ARF}$ whether at a basal level or after incubation with TGFβ1.

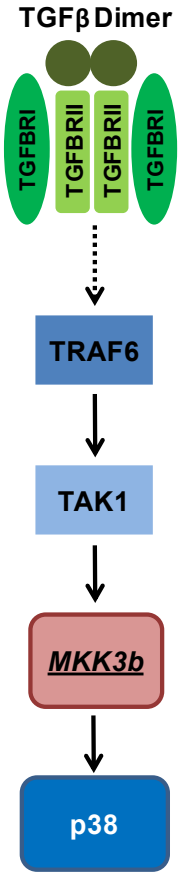

Figure 3.6: Diagram of non-canonical TGFβI activation of p38. The dimeric TGFβ signaling ligand activates and stabilizes formation of the TGFβR complex. TRAF6 is recruited and binds to (dotted line) activated TGFβR. TAK1 interacts with TRAF6 allowing it to be phosphorylated by TGFβRI. Upon release, TRAF6 proceeds to activate MKK3b, the long isoform of MKK3. MKK3b can then directly interact with and phosphorylate p38 which goes on to activate a context specific transcriptional program.

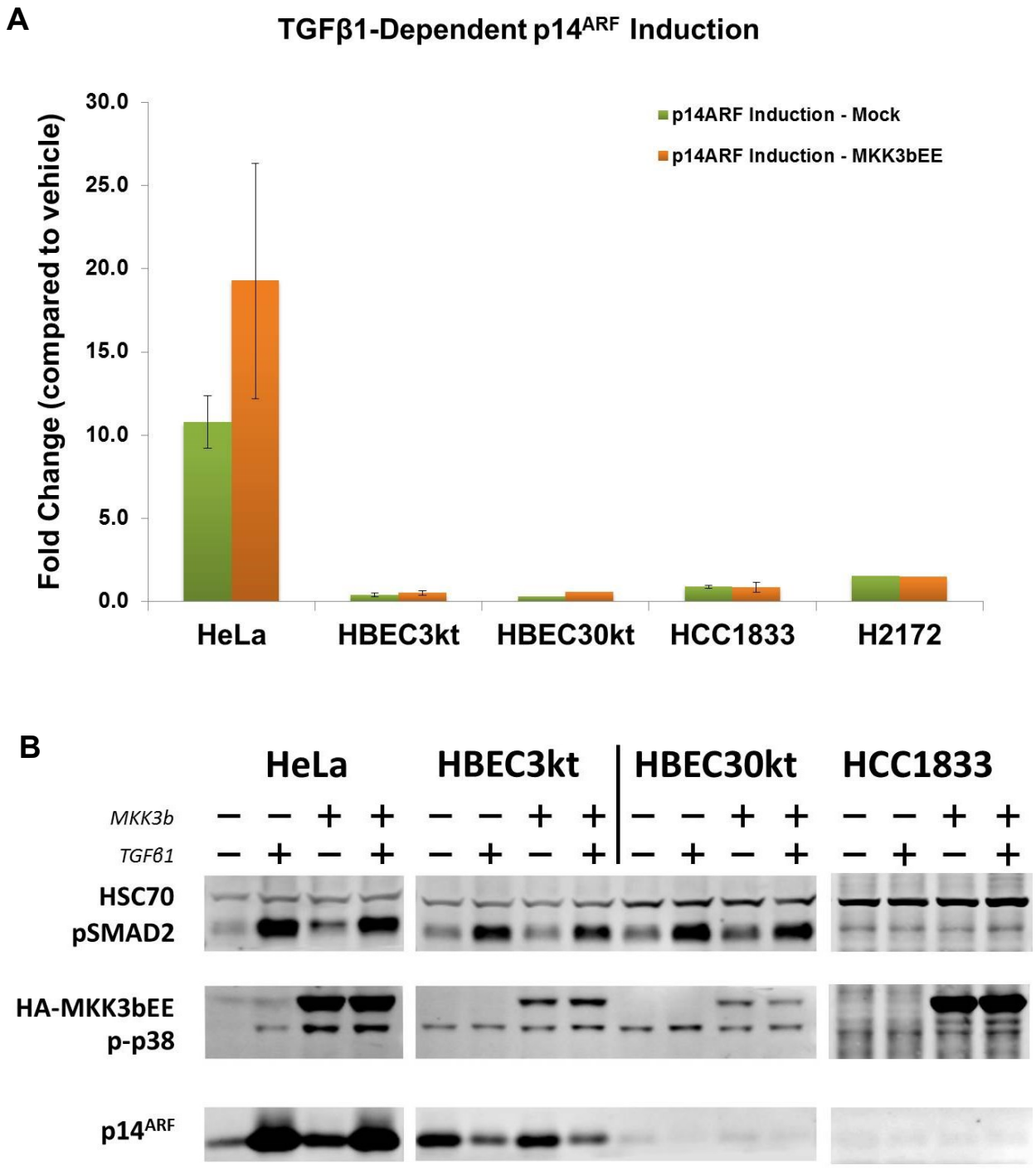

Figure 3.7: Ectopic expression of MKK3b does not increase TGFβl-dependent *ARF* induction. A) A representative western blot demonstrating that even upon transfection of constitutively active MKK3b and subsequent forced activation of p38, $p14^{ARF}$ levels remain unaffected both in the absence and presence of TGFβ1. B) Quantification of 3 separate transfections (HBEC30kt and H2172 are an n=1) demonstrating these results are consistent among biological replicates. $p14^{ARF}$ levels were normalized to HSC70 and then compared to vehicle treated cells to measure fold change.

Concluding Remarks

The importance of SMAD2/3 and p38 activation for the induction of *ARF* in response to TGFβ has been well demonstrated by the Skapek lab in MEFs and HeLa cells. Translating these findings to NSCLC, I was unable to identify lines that had intact *ARF* and induced its expression in response to TGFβ1, whether transcriptionally or translationally. I was able to establish a timeline for activation of SMAD2 and p38, two important mediators in TGFβ-dependent induction of *ARF* for HeLa cells. By observing the activation patterns for these proteins in the NSCLC cell line panel, I found potential defects in the signaling pathway.

In an attempt to restore TGFβ-dependent *ARF* induction, I overexpressed a mutant form of p38 activation MKK3b. Though many cell lines showed increased p38 phosphorylation, I was not able to increase or restore $p14^{ARF}$ expression. Despite this outcome, there were some cell lines that had initially failed to activate SMAD2 upon TGFβ1 treatment, opening the possibility that a constitutively active mutant of SMAD2 and/or ectopic expression of co-SMAD4 could lead to induction of *ARF*.

Intriguingly, despite there not being a clear induction of *ARF* in the NSCLC lines, the immortalized HBEC cells consistently showed decreased *ARF* expression in response to TGFβ1. This demonstrates that TGFβ1 stimulation may affect ARF expression in a cell type dependent manner.. This finding could be of interest when trying to understand TGFβ-dependent *ARF* induction.

It is known that in HeLa cells, the HPV proteins E6 and E7 are expressed, inhibiting p53 and RB1 expression respectively. To test if p53 inhibition was necessary for *ARF* induction, I used immortalized human foreskin (BJ) cells stably transfected with a plasmid expressing

E6/E7. Compared to non-transfected cells, I did not observe an increase in $p14^{ARF}$ in response to TGFβ1 though basal levels were increased in the transfected line. I did not include this data here as I was not able to confirm expression of E6/E7 in either the transfected cells or HeLa cells. In addition to these data, Dr. Yanbin Zheng in the Skapek lab has shown that knockdown of the E6/E7 proteins in HeLa cells does not affect induction of *ARF* in response to TGFβ.

CHAPTER 4:

Transcriptional Regulation of *ARF* in Response to TGFβ-I

Introduction

Mechanisms of POLR2A transcriptional regulation

The role of POLR2A in mRNA transcription is essential and so it is not surprising that there are different mechanisms in which its activity can be regulated to control gene expression (reviewed in Fuda et al., 2009). Though there are many steps required for successful initiation of transcription, most genes can be classified by the status of POLR2A at the promoter. The minimum requirement is that the promoter is accessible and that the preinitiation complex (PIC; consisting of other factors including POLR2A) is present, so that genes lacking POLR2A are considered to be in an off state (Fig 4.1).

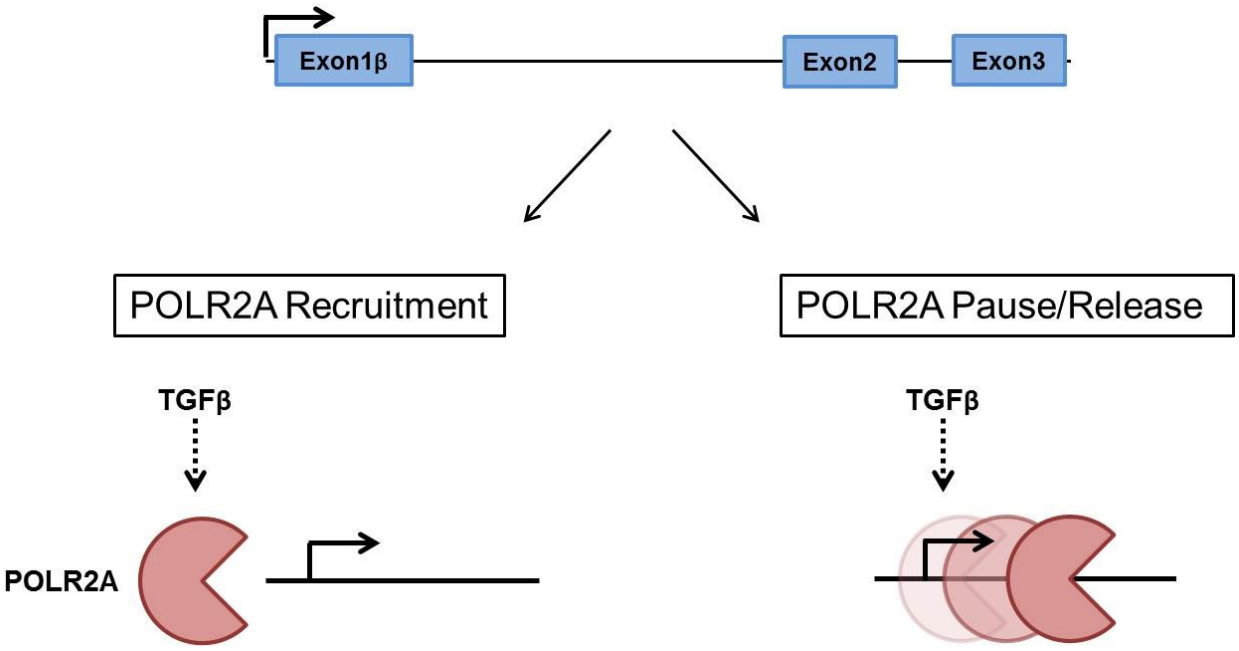

Figure 4.1: Diagram of the two states of POLR2A association to *ARF* promoter. POLR2A can be regulated by two broad mechanisms. For some genes, POLR2A can be physically recruited to the promoter, such as what has been observed for *ARF* in MEFs. In contrast, POLR2A can already be present at a gene promoter and held in an inactive or paused state until released.

Though POLR2A might occupy the promoter of a gene, this does not mean that it proceeds to transcribe mRNA. In addition to PIC assembly, POLR2A can be held in a paused state at the promoter as determined by whether the C-terminal domain (CTD), which is composed of a repeated heptapeptide sequence, is phosphorylated along with presence of certain cofactors. Many genes have POLR2A present but do not show active transcription until these cofactors are assembled and the CTD is phosphorylated. For example p-TEFb, which includes CDK9, must be recruited to phosphorylate negative elongation factor (NELF) and serine 5 in the CTD before full transcription can proceed (Fig 4.2). These steps are initiated in response to the appropriate stimuli, such as TGFβ and other growth factors, and recruitment of coactivators.

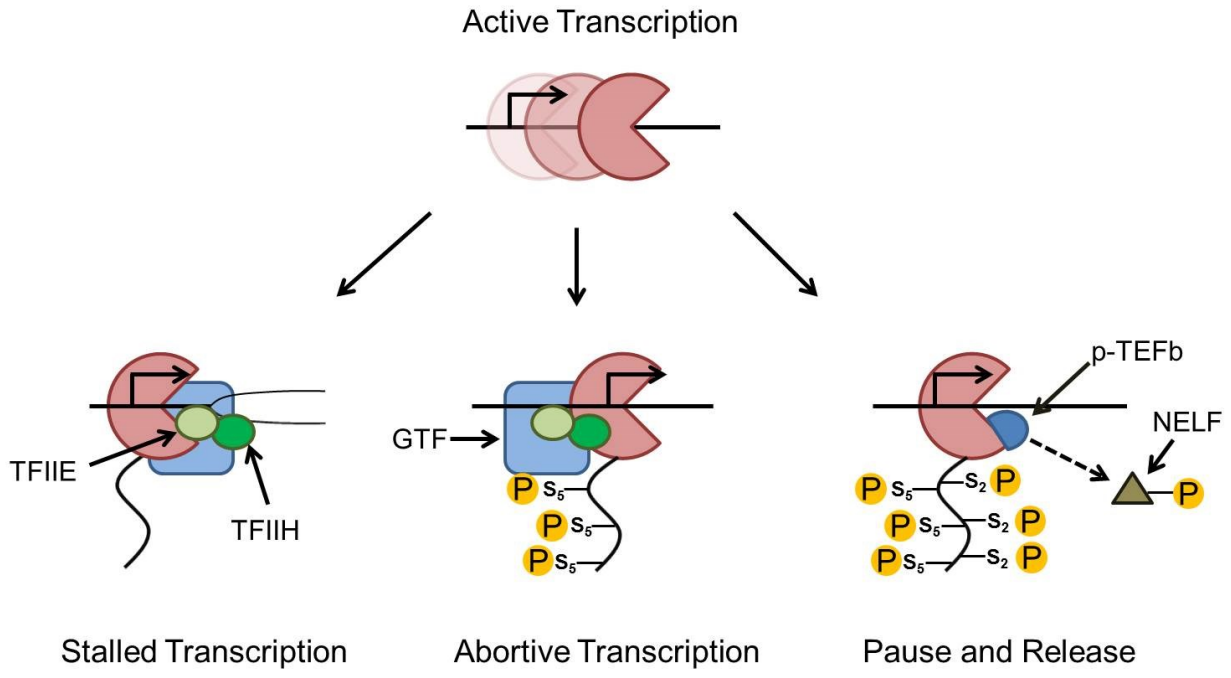

Figure 4.2: Diagram of the multiple methods of regulation for POLR2A already present at a gene promoter. To initiate active transcription, multiple different steps must be happen. Two of the initial general transcription factors (GTFs) need to be recruited. TFIIE facilitates the separation of dsDNA while TFIIH phosphorylates serine 5 in the CTD of POLR2A. After the GTFs prepare DNA and POLR2A for active transcription, if they do not dissociate from the complex then transcript synthesis will be aborted shortly after. Once p-TEFb, a complex which includes CDK9, associates with POLR2A to phosphorylate both NELF and serine 2 in the CTD, NELF dissociates from the complex and POLR2A is released from a paused state.

Transcriptional response at the Arf promoter in response to TGFβ

When I started this project, I made a decision to investigate complex mechanisms in which TGFβ induces *ARF* expression and whether I could identify faults in this pathway. Taking a step back, I decided to address a basic, fundamental question of what happens at the *ARF* promoter itself. The Skapek lab had previously shown that in MEFs, Polr2a is recruited to the proximal promoter after 24hr in the presence of Tgfβ2, the same timepoint that increases in transcript levels are detected, demonstrating that increase in *Arf* expression positively correlates with increased Polr2a occupation (Fig 4.2) (Zheng et al., 2010). I have shown previously that in HeLa cells, *ARF* transcript and protein levels increase at the 24 hr timepoint after treatment with TGFβ1. This led to the question that is it only TGFβ-dependent *ARF* transcript and protein induction that is identical in HeLa, or is POLR2A recruited in a similar fashion to MEFs.

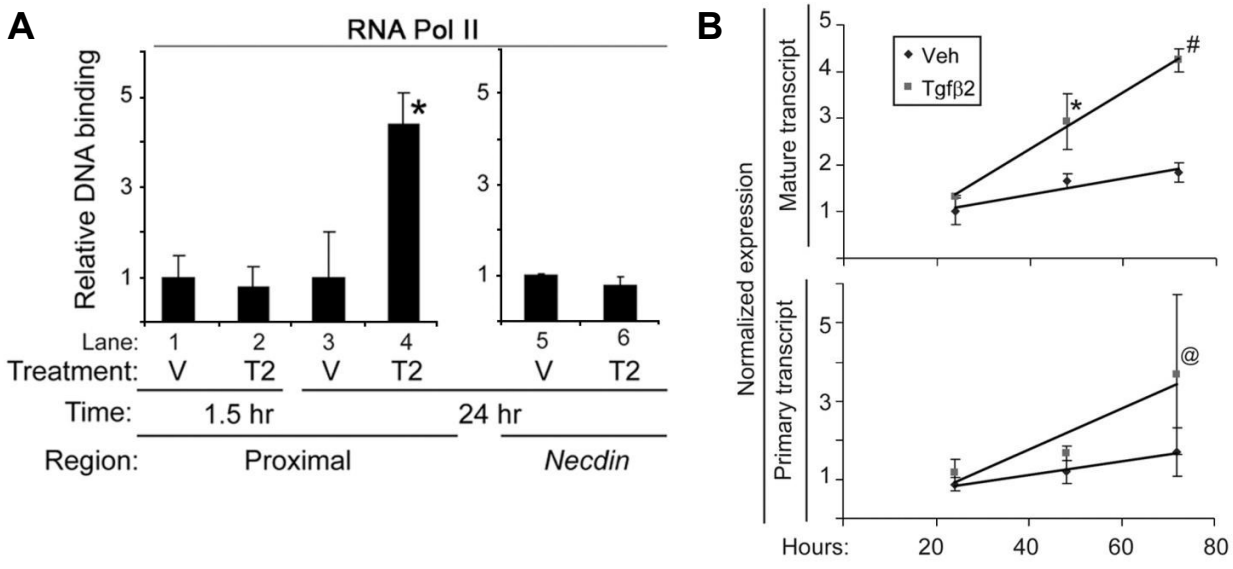

Figure 4.3: Polr2a is recruited to the *Arf* promoter in MEFs at 24 hr. A) In Tgfβ2 treated MEFs, ChIP for Polr2a demonstrates that recruitment increases significantly after 24 hr. B) This recruitment of Polr2a is at the same timepoint that increases in both primary and mature *Arf* transcript can be observed by RT-qPCR (modified from Zheng et al., 2010).

In addition to data demonstrating that in MEFs *Arf* induction and Polr2A recruitment is delayed in response to Tgfβ2, the Skapek lab showed that Smad2/3 is recruited to the promoter within 1.5 hr of treatment with Tgfβ2. This is an interesting observation as it shows that while Smad2/3 is recruited to the promoter of *Arf* early in response to Tgfβ, Polr2a recruitment does not take place until increases in transcript levels are detectable. What this suggests is that there was another mode of regulation independent of Smad2/3 activation. Using these data, I asked whether these same changes occur in HeLa cells in addition to how these changes compared to HCC1833, a cell line that activates SMAD2 in response to TGFβ, but does not induce *ARF*.

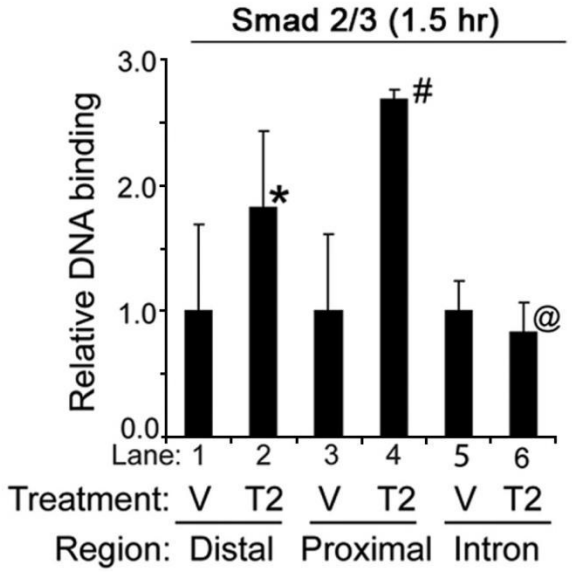

Figure 4.4: Smad2/3 binds at the proximal promoter of *Arf* within 90 min of Tgfβ2 treatment. In MEFs, ChIP for Smad2/3 binding shows that binding to the *Arf* proximal promoter occurs quickly, within 90 min after incubation with Tgfβ2. This is in contrast to the delayed recruitment of Polr2a to same region (modified from Zheng et al., 2010).

Methods

Cell lines

HeLa and HCC1833 cell lines were cultured as described previously in chapter 3. Cells were cultured and split into 10 cm culture plates and allowed to adhere overnight. The following day, cells were treated with either TGFβ1 or vehicle in fresh media, at concentrations previously described, for 0 or 24 hr. Cells were harvested on plate after washing twice with cold, 1X PBS.

Primer design and validation

Primers were designed for the first intron of *ARF*, the promoter region of POLR2A, and a gene desert region within the short arm of chromosome 4. Primers were validated by both PCR and qPCR using HeLa genomic DNA to ensure specificity. For primer list, see appendix.

Chromatin immunoprecipitation

HeLa and HCC1833 cells were treated with either TGFβ1 at a final concentration of 5 ng/mL or equivalent volume of vehicle (10μM HCl, 25μg/mL BSA) for 24 hr. After incubation, cells were harvested and ChIP was performed according to the manufacture's protocol (Santa Cruz; Protein A/G PLUS-Agarose).

Real-time quantitative PCR and western blotting

Both techniques were carried out as outlined in chapter 4 with the exception that qPCR was not subject to reverse transcriptase treatment due to genomic DNA being used.

Results

POLR2A occupancy at the ARF promoter does not increase in response to TGFβ1

I used ChIP with a POLR2A specific antibody to observe whether recruitment was increased in the presence of TGFβ1 as compared to vehicle treated HeLa and HCC1833 cells. In addition, I measured POLR2A occupancy at the first intron of *ARF* while using the *POLR2A* promoter as the positive control and a gene desert region (GDR) in the short arm of chromosome 4 as the negative control. There was no POLR2A recruitment observed for HeLa and HCC1833 cells after incubating for 24 hr with TGFβ1 (Fig 4.4). Interestingly, POLR2A occupancy levels decreased at the *ARF* promoter in HeLa while levels at the first *ARF* intron

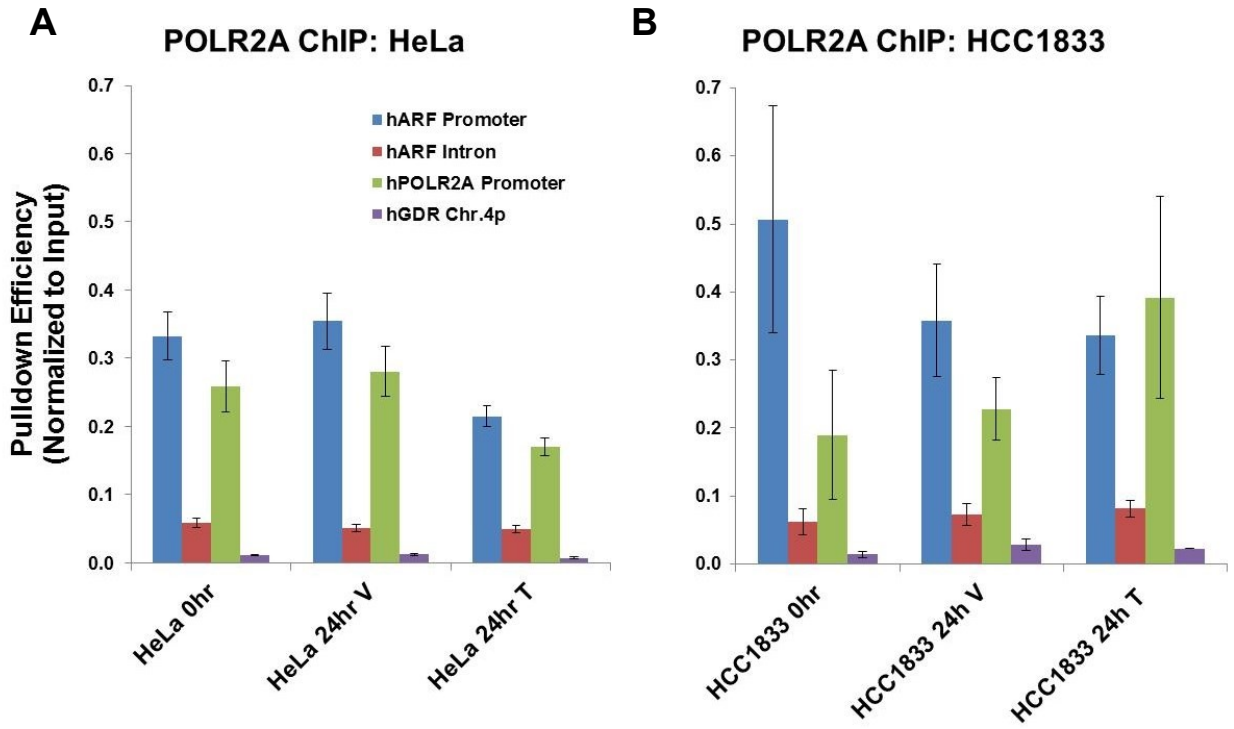

Figure 4.4: POLR2A occupancy at *ARF* promoter does not increase in response to TGFβI. A) In HeLa cells, ChIP for POLR2A does not show increased occupancy after 24 hr of incubation with TGFβ1 though overall occupancy at all regions except for the first of *Arf* decreases. B) HCC1833 cells do not show significant POLR2A changes at any region in response to TGFβ1 after 24 hr when compared to vehicle treated cells at the same timepoint.

remained the same (Fig 4.4A). Furthermore in HCC1833, basal POLR2A occupancy levels at the *ARF* promoter were similar to that observed in HeLa cells.

To better visualize the dynamics of POLR2A occupancy, I compared the relative levels at the *ARF* promoter and first *ARF* intron for HeLa and HCC1833. In TGFβ1 treated HeLa cells, there is a significant increase in the relative amount of POLR2A at the first intron of *ARF* compared to the promoter. In HCC1833 which shows SMAD2 activation in response to TGFβ1 but *ARF* expression is not induced, no change was observed. Together these data demonstrate that in HeLa there is a positive correlation in the relative amount of POLR2A at the first intron of *ARF* in response to TGFβ1 while HCC1833, a cell line in which *ARF* is not induced, this correlation does not exist.

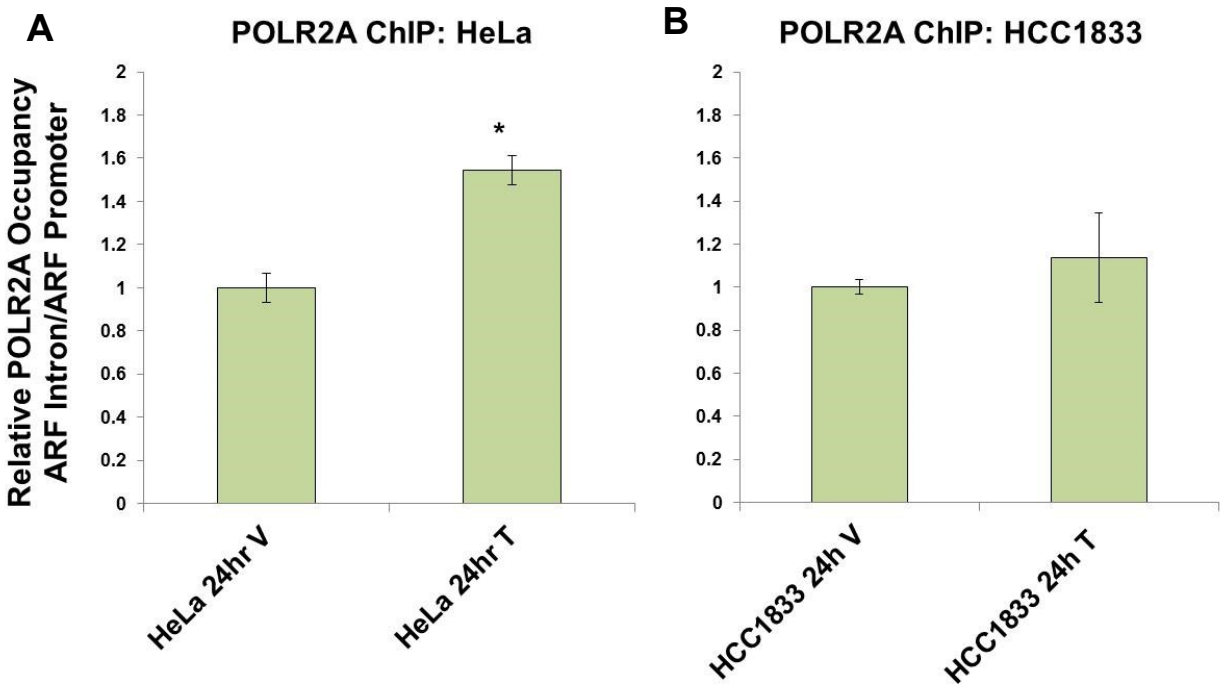

Figure 4.5: TGFβ1 increases the relative amount of POLR2A at the first intron. A) When compared to the occupancy at the *ARF* promoter, the amount of POLR2A increases at the first intron of *ARF* in response to TGFβ1 in HeLa cells at 24 hr. B) In contrast to HeLa cells, HCC1833 cells show no significant increase in relative amounts of POLR2A. (*) $p<0.05$

Concluding Remarks

I have shown that in contrast to MEFs, HeLa cells do not demonstrate POLR2A recruitment in response to TGFβ as a mechanism of direct transcriptional regulation of *ARF*. This preliminary data suggests that for HeLa cells, the induction of *ARF* in response to TGFβ is regulated in part by POLR2A being released from a paused state to initiate processive transcription. Though there is a decrease in the occupancy of POLR2A at its own promoter, this has been previously observed by others in response to signaling factors (Kininis et al., 2009).

To confirm these findings, it is important to expand the interrogation of POLR2A occupancy across the *ARF* locus in addition to other reference genes, the ideal method to pursue this being ChIP-seq. It is known that POLR2A occupancy can vary greatly even at basal levels in many genes (reviewed here Adelman and Lis, 2012). This could indicate why there is not a significant increase in POLR2A occupancy at the first intron of *ARF*.

In addition to mapping changes in POLR2A in response to TGFβ, investigating the phosphorylation states of the CTD will provide additional support to a pause and release mechanism. Using antibodies targeting phosphorylated serine 5, it would be hypothesized that this modification is not present until after incubation with TGFβ. This could be further verified through observing CDK9 recruitment, indicating that p-TEFb has been assembled along with POLR2A in the active transcriptional complex.

CHAPTER 5:

Discussion and Future Directions

In an attempt to better understand the mechanisms by which TGFβ induces *ARF*, I first set out to identify distal, *cis* acting regulatory elements in the mouse orthologous 9p21.3 CAD risk locus. Even though technical issues prevented me from gathering data definitely showing interaction in conserved sequences in the risk locus with the *Arf* promoter, *BglII* digest efficiencies did indicate that regions within the risk locus were more accessible, and thus open, than others suggesting that this region could contain important regulatory elements. In addition to these data, when translating data from the Skapek lab from HeLa to a panel of NSCLC cells, I was able to determine a pattern for TGFβ signaling that led to *ARF* induction in HeLa. Furthermore, forcing activation of p38 did not result in induction or increased $p14^{ARF}$ levels, showing that p38 is necessary but not sufficient for *ARF* induction. At the *ARF* promoter, I have shown that TGFβ is not responsible for the recruitment of POLR2A as is seen in MEFs, but that it is involved in the release of POLR2A from a paused state to induce transcription.

In further exploration of the 9p21.3 CAD risk locus, it would be prudent to approach the preliminary identification of potential regulatory elements using a non-biased approach in

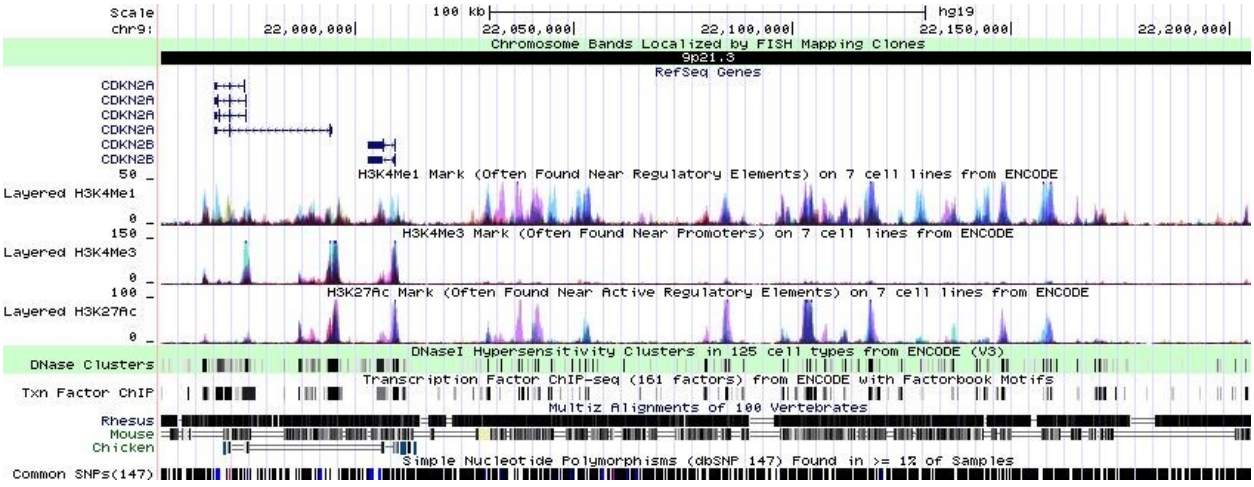

Figure 5.1: The 9p21.3 CAD risk interval contains enhancer associated chromatin modifications. Histone marks, as measured by ChIP-seq, indicative of enhancer elements are found at high levels within the 9p21.3 CAD risk interval in humans. These marks are in addition to transcription factor and DNase clusters displaying open regions within the risk locus at which many different transcription factor binding sites can be found (Benson et al., 2013; Galperin et al., 2015; Kent et al., 2002; Lander et al., 2001).

contrast to my first attempt. Mapping by the ENCODE project clearly shows that regions within the risk locus are open and contain histone modifications indicative of enhancer elements (Fig 5.1) (Benson et al., 2013; Galperin et al., 2015; Kent et al., 2002; Lander et al., 2001). Others have shown that this region can interact with the *CDKN2A*/*ARF*/*CDKN2B* locus in response to interferon-γ and that certain SNPs impair this (Harismendy et al., 2011). Thus one approach towards identifying *cis*-acting regulatory elements would be by using ChIP-seq analysis of histone markers in the 9p21.3 CAD risk locus that are indicative of enhancer regions (e.g. H3K4me3 and H3K27ac) and if/how these marks change in response to TGFβ.

Though I have established the timing of activation of SMAD2 and p38, along with p38's necessity but not sufficiency in *ARF* induction, there remains many components of the TGFβ pathway that have not been explored in regards to activation and involvement. There are a plethora of resources available to study TGFβ signaling, including ELISA protein arrays used to detect phosphorylation of proteins downstream of the receptor, allowing for a better characterization of the signaling involved. In addition to ELISA arrays, siRNA libraries specifically focusing on TGFβ pathway proteins and targets could be used in conjunction or separately to observe what proteins are necessary for *ARF* induction, for example using HeLa cells in a 384-well plate siRNA screen. These experiments would add a vast amount of knowledge to the intricacies involved between TGFβ receptor activation and the eventual binding of the transcriptionally active SMAD complex to the *ARF* promoter.

As I have shown the preliminary evidence for POLR2A pause and release in response to TGFβ1 leading to induction of *ARF*, a clear path forward is to firmly establish this mechanism. In addition to the sites that were assayed for POLR2A occupancy, expanding both control regions and the *ARF* locus itself by using ChIP-seq would provide a comprehensive view of POLR2A processivity increase in response to TGFβ. As I described in the conclusion to chapter 4, there

remains the open questions of what changes in phosphorylation occur at the C-terminal domain of POLR2A which could be determined by using ChIP antibodies specific for these different modifications and how they change at different time points. Intimately tied to these changes in phosphorylation states is the recruitment of the p-TEFb complex containing CDK9, providing further ChIP targets in the same experimental approach as the C-terminal domain of POLR2A.

The regulation and expression of *ARF* remains an important area of research, especially when considering its role in cell cycle arrest and tumor suppression. Though the effects of *Arf* loss and cancer progression in mice are clear, these same effects have been harder to elucidate in humans. As the focus of my dissertation work, I have attempted to clarify TGFβ's role in *ARF* expression at both protein signaling and transcriptional levels of regulation. This research contributes to the understanding of *ARF* induction and works toward the ultimate goal of utilizing this knowledge to open new therapeutic options towards cancer treatment.

APPENDIX

Table 1A: Primers used for 3C experiment.

Name	Sequence (5'-3')	Target	Product Size
p19Arf-Con 2	TTCTGTGTCTGAAGTGCA	1st *BglII* Site US of *Arf*	
CNS1-UpSt 2.2	ACCTGAGTGTAGATTCCCAG	1st *BglII* Site US of CNS1	155
CNS2-Upst 2.2	TCTGAAAGCTAGATTTACAAGG	1st *BglII* Site US of CNS2	118
CNS3-Upst 2.1	ACTATTCTTTCAGCATCCTC	*BglII* Site US of CNS3	121
CNS3-Mid 2.1	CACAGTTTCAAGTTCCAGATG	*BglII* Site in CNS3	113
CNS4-Upst 2.1	CAGATGCAGAAAGACCAACC	*BglII* Site US of CNS4	146
CNS4-Mid3 2.1	CATGAGATTCGGGAGTCAAG	3rd US *BglII* Site in CNS4	115
Gapdh1	CTTCATCTGCCTCCCTAAG	Internal *Gapdh BglII* Site	
Gapdh2	ACACAGGCAAAATACCAATG		
Gapdh3	CTGCGCCTCAGAATCCTG		
Gapdh4	GAATGCTTGGATGTACAACC		
Gapdh-F1	ACAGTCCATGCCATCACTGCC	*Gapdh* Loading Control	266
Gapdh-R1	GCCTGCTTCACCACCTTCTTG		

Table 2A: Primers used for 3C *BglII* digest efficiency experiments.

Name	Sequence (5'-3')	Target	Product Size
p19Arf-Con 1	CTGGCCTCTCTGCTTCTG	1st *BglII* Site us of *Arf*	597
Arf Con1 Fwd	TGGTGGCAAGGGAGGAAATC		
CNS1-UpSt 2.2	ACCTGAGTGTAGATTCCCAG	1st *BglII* Site US of CNS1	469
CNS1-U-2.2 Fwd	TGATCTAAGTGCCTTCCCAC		
CNS2-Upst 2.2	TCTGAAAGCTAGATTTACAAGG	1st *BglII* Site US of CNS2	342
CNS2-U-2.2 Fwd	AAAGAGCCAGTACAGTACGG		
CNS3-Upst 2.1	ACTATTCTTTCAGCATCCTC	*BglII* Site US of CNS3	260
CNS3-U-2.1 Fwd	CCCATCTGTTTGTAACTCCA		
CNS3-Mid 2.1	CACAGTTTCAAGTTCCAGATG	*BglII* Site in CNS3	373
CNS3-M-2.1 Fwd	CTTCCGAAAACAGTGTCCAT		
CNS4-Upst 2.1	CAGATGCAGAAAGACCAACC	*BglII* Site US of CNS4	232
CNS4-U-2.1 Fwd	GTTGTTCTCCCTCCTTGCTC		
CNS4-Mid3 2.1	CATGAGATTCGGGAGTCAAG	3rd US *BglII* Site in CNS4	336

CNS4-M3-2.1 Fwd	AACTCTGCGTGTGTCTCTTC		
CNS4-Mid4 1.2	TACTGACCATCTTGCCTTCC	4th *BglII* Site US of CNS4	447
CNS4-M4-1.2 Fwd	CACGGTCAGGTTTGTCACAG		
Gapdh1F	CTTCATCTGCCTCCCTAAG		171
Gapdh1R	ACACAGGCAAAATACCAATG		
Gapdh3F	CTGCGCCTCAGAATCCTG		669
Gapdh3R	GAATGCTTGGATGTACAACC		

Table 3A: Primers used for confirming presence of *ARF* exons in human cell line panel.

Name	Sequence (5'-3')	Product Size
p14 ARF Exon 1B 226 S	CCGCGTGCGCAGGGCTCAG	341
p14 ARF Exon 1B 226 AS	CGCGGGATGTGAACCACGAAAAC	
p14 ARF Exon 2 S	GTGGGGGTCTGCTTGGCGGTGAG	570
p14 ARF Exon 2 AS	TGGCGGGGCAGGGCGATAG	
p14 ARF Exon 3-1 S	CGCCTGTTTTCTTTCTGCCCTCT	431
p14 ARF Exon 3-1 AS	CCCCCTGAGCTTCCCTAGTTCAC	

Table 4A: Primers used for POLR2A recruitment and occupancy ChIP experiments.

Name	Sequence (5'-3')	Target	Product Size
hARFprox-2F	ACACAGGGCGGGAAAGTG	*ARF* Prox Promoter	142
hARFprox-2R	GACCTCCAAGATCTCGGAAC		
hARFintr-1F	TGCTCTTACCACCCACATTG	*ARF* 1st intron	91
hARFintr-1R	ATTGTGGTTTAGCCCCGAAG		
hPOL2pro-1F	GCTGAAGATGAAACCGTTGTC	*POLR2A* Promoter region	82
hPOL2pro-1R	GCGACCTTTTGAAGTGACAG		
hGAPDHpro-3F	CAACTTTCCCGCCTCTCAG	*GAPDH* Promoter region	138
hGAPDHpro-3R	ACACGCTTGGATGAAACAGG		
hGDRchr4p-2F	CCATTTCCTTGGGGCTTCTG	Gene Desert Region: Chromosome 4p	139
hGDRchr4p-2R	ATGAGCAGTGAGAGGTCAGG		

REFERENCES

Adelman, K., and Lis, J.T. (2012). Promoter-proximal pausing of RNA polymerase II: emerging roles in metazoans. Nat Rev Genet *13*, 720-731.

Anzano, M.A., Roberts, A.B., Meyers, C.A., Komoriya, A., Lamb, L.C., Smith, J.M., and Sporn, M.B. (1982). Synergistic interaction of two classes of transforming growth factors from murine sarcoma cells. Cancer Res *42*, 4776-4778.

Bates, S., Phillips, A.C., Clark, P.A., Stott, F., Peters, G., Ludwig, R.L., and Vousden, K.H. (1998). p14ARF links the tumour suppressors RB and p53. Nature *395*, 124-125.

Benson, D.A., Cavanaugh, M., Clark, K., Karsch-Mizrachi, I., Lipman, D.J., Ostell, J., and Sayers, E.W. (2013). GenBank. Nucleic Acids Res *41*, D36-42.

Cheng, J.Q., Jhanwar, S.C., Lu, Y.Y., and Testa, J.R. (1993). Homozygous deletions within 9p21-p22 identify a small critical region of chromosomal loss in human malignant mesotheliomas. Cancer Res *53*, 4761-4763.

Cowan, J.M., Halaban, R., and Francke, U. (1988). Cytogenetic analysis of melanocytes from premalignant nevi and melanomas. J Natl Cancer Inst *80*, 1159-1164.

de Larco, J.E., and Todaro, G.J. (1978). Growth factors from murine sarcoma virus-transformed cells. Proc Natl Acad Sci U S A *75*, 4001-4005.

Dekker, J., Rippe, K., Dekker, M., and Kleckner, N. (2002). Capturing chromosome conformation. Science *295*, 1306-1311.

Diaz, M.O., Rubin, C.M., Harden, A., Ziemin, S., Larson, R.A., Le Beau, M.M., and Rowley, J.D. (1990). Deletions of interferon genes in acute lymphoblastic leukemia. N Engl J Med *322*, 77-82.

Diaz, M.O., Ziemin, S., Le Beau, M.M., Pitha, P., Smith, S.D., Chilcote, R.R., and Rowley, J.D. (1988). Homozygous deletion of the alpha- and beta 1-interferon genes in human leukemia and derived cell lines. Proc Natl Acad Sci U S A *85*, 5259-5263.

Eymin, B., Karayan, L., Seite, P., Brambilla, C., Brambilla, E., Larsen, C.J., and Gazzeri, S. (2001). Human ARF binds E2F1 and inhibits its transcriptional activity. Oncogene *20*, 1033-1041.

Fountain, J.W., Karayiorgou, M., Ernstoff, M.S., Kirkwood, J.M., Vlock, D.R., Titus-Ernstoff, L., Bouchard, B., Vijayasaradhi, S., Houghton, A.N., Lahti, J.*, et al.* (1992). Homozygous deletions within human chromosome band 9p21 in melanoma. Proc Natl Acad Sci U S A *89*, 10557-10561.

Freeman-Anderson, N.E., Zheng, Y., McCalla-Martin, A.C., Treanor, L.M., Zhao, Y.D., Garfin, P.M., He, T.C., Mary, M.N., Thornton, J.D., Anderson, C.*, et al.* (2009). Expression of the Arf tumor suppressor gene is controlled by Tgfbeta2 during development. Development *136*, 2081-2089.

Fuda, N.J., Ardehali, M.B., and Lis, J.T. (2009). Defining mechanisms that regulate RNA polymerase II transcription in vivo. Nature *461*, 186-192.

Galperin, M.Y., Rigden, D.J., and Fernandez-Suarez, X.M. (2015). The 2015 Nucleic Acids Research Database Issue and molecular biology database collection. Nucleic Acids Res *43*, D1-5.

Hagege, H., Klous, P., Braem, C., Splinter, E., Dekker, J., Cathala, G., de Laat, W., and Forne, T. (2007). Quantitative analysis of chromosome conformation capture assays (3C-qPCR). Nat Protoc *2*, 1722-1733.

Hall, M., and Peters, G. (1996). Genetic alterations of cyclins, cyclin-dependent kinases, and Cdk inhibitors in human cancer. Adv Cancer Res *68*, 67-108.

Hannon, G.J., and Beach, D. (1994). p15INK4B is a potential effector of TGF-beta-induced cell cycle arrest. Nature *371*, 257-261.

Harismendy, O., Notani, D., Song, X., Rahim, N.G., Tanasa, B., Heintzman, N., Ren, B., Fu, X.D., Topol, E.J., Rosenfeld, M.G.*, et al.* (2011). 9p21 DNA variants associated with coronary artery disease impair interferon-gamma signalling response. Nature *470*, 264-268.

Hirama, T., and Koeffler, H.P. (1995). Role of the cyclin-dependent kinase inhibitors in the development of cancer. Blood *86*, 841-854.

James, C.D., He, J., Collins, V.P., Allalunis-Turner, M.J., and Day, R.S., 3rd (1993). Localization of chromosome 9p homozygous deletions in glioma cell lines with markers constituting a continuous linkage group. Cancer Res *53*, 3674-3676.

Jarinova, O., Stewart, A.F., Roberts, R., Wells, G., Lau, P., Naing, T., Buerki, C., McLean, B.W., Cook, R.C., Parker, J.S.*, et al.* (2009). Functional analysis of the chromosome 9p21.3 coronary artery disease risk locus. Arterioscler Thromb Vasc Biol *29*, 1671-1677.

Jeck, W.R., Siebold, A.P., and Sharpless, N.E. (2012). Review: a meta-analysis of GWAS and age-associated diseases. Aging Cell *11*, 727-731.

Kamb, A., Gruis, N.A., Weaver-Feldhaus, J., Liu, Q., Harshman, K., Tavtigian, S.V., Stockert, E., Day, R.S., 3rd, Johnson, B.E., and Skolnick, M.H. (1994). A cell cycle regulator potentially involved in genesis of many tumor types. Science *264*, 436-440.

Kamijo, T., Zindy, F., Roussel, M.F., Quelle, D.E., Downing, J.R., Ashmun, R.A., Grosveld, G., and Sherr, C.J. (1997). Tumor suppression at the mouse INK4a locus mediated by the alternative reading frame product p19ARF. Cell *91*, 649-659.

Kent, W.J., Sugnet, C.W., Furey, T.S., Roskin, K.M., Pringle, T.H., Zahler, A.M., and Haussler, D. (2002). The human genome browser at UCSC. Genome Res *12*, 996-1006.

Kininis, M., Isaacs, G.D., Core, L.J., Hah, N., and Kraus, W.L. (2009). Postrecruitment regulation of RNA polymerase II directs rapid signaling responses at the promoters of estrogen target genes. Mol Cell Biol *29*, 1123-1133.

Lander, E.S., Linton, L.M., Birren, B., Nusbaum, C., Zody, M.C., Baldwin, J., Devon, K., Dewar, K., Doyle, M., FitzHugh, W.*, et al.* (2001). Initial sequencing and analysis of the human genome. Nature *409*, 860-921.

Lebrun, J.-J. (2012). The Dual Role of TGF in Human Cancer: From Tumor Suppression to Cancer Metastasis. ISRN Molecular Biology *2012*, 28.

Levy, L., and Hill, C.S. (2006). Alterations in components of the TGF-beta superfamily signaling pathways in human cancer. Cytokine Growth Factor Rev *17*, 41-58.

Lukeis, R., Irving, L., Garson, M., and Hasthorpe, S. (1990). Cytogenetics of non-small cell lung cancer: analysis of consistent non-random abnormalities. Genes Chromosomes Cancer *2*, 116-124.

Martin, A.C., Thornton, J.D., Liu, J., Wang, X., Zuo, J., Jablonski, M.M., Chaum, E., Zindy, F., and Skapek, S.X. (2004). Pathogenesis of persistent hyperplastic primary vitreous in mice lacking the arf tumor suppressor gene. Invest Ophthalmol Vis Sci *45*, 3387-3396.

Massague, J., Seoane, J., and Wotton, D. (2005). Smad transcription factors. Genes Dev *19*, 2783-2810.

McKeller, R.N., Fowler, J.L., Cunningham, J.J., Warner, N., Smeyne, R.J., Zindy, F., and Skapek, S.X. (2002). The Arf tumor suppressor gene promotes hyaloid vascular regression during mouse eye development. Proc Natl Acad Sci U S A *99*, 3848-3853.

McPherson, R., Pertsemlidis, A., Kavaslar, N., Stewart, A., Roberts, R., Cox, D.R., Hinds, D.A., Pennacchio, L.A., Tybjaerg-Hansen, A., Folsom, A.R.*, et al.* (2007). A common allele on chromosome 9 associated with coronary heart disease. Science *316*, 1488-1491.

Merlo, A., Gabrielson, E., Askin, F., and Sidransky, D. (1994). Frequent loss of chromosome 9 in human primary non-small cell lung cancer. Cancer Res *54*, 640-642.

Middleton, P.G., Prince, R.A., Williamson, I.K., Taylor, P.R., Reid, M.M., Jackson, G.H., Katz, F., Chessells, J.M., and Proctor, S.J. (1991). Alpha interferon gene deletions in adults, children and infants with acute lymphoblastic leukemia. Leukemia *5*, 680-682.

Miele, A., Gheldof, N., Tabuchi, T.M., Dostie, J., and Dekker, J. (2006). Mapping chromatin interactions by chromosome conformation capture. Curr Protoc Mol Biol *Chapter 21*, Unit 21 11.

Mori, S., Ito, G., Usami, N., Yoshioka, H., Ueda, Y., Kodama, Y., Takahashi, M., Fong, K.M., Shimokata, K., and Sekido, Y. (2004). p53 apoptotic pathway molecules are frequently and simultaneously altered in nonsmall cell lung carcinoma. Cancer *100*, 1673-1682.

Naumova, N., Smith, E.M., Zhan, Y., and Dekker, J. (2012). Analysis of long-range chromatin interactions using Chromosome Conformation Capture. Methods *58*, 192-203.

Nobori, T., Miura, K., Wu, D.J., Lois, A., Takabayashi, K., and Carson, D.A. (1994). Deletions of the cyclin-dependent kinase-4 inhibitor gene in multiple human cancers. Nature *368*, 753-756.

Olopade, O.I., Buchhagen, D.L., Malik, K., Sherman, J., Nobori, T., Bader, S., Nau, M.M., Gazdar, A.F., Minna, J.D., and Diaz, M.O. (1993). Homozygous loss of the interferon genes defines the critical region on 9p that is deleted in lung cancers. Cancer Res *53*, 2410-2415.

Olopade, O.I., Jenkins, R.B., Ransom, D.T., Malik, K., Pomykala, H., Nobori, T., Cowan, J.M., Rowley, J.D., and Diaz, M.O. (1992). Molecular analysis of deletions of the short arm of chromosome 9 in human gliomas. Cancer Res *52*, 2523-2529.

Palmero, I., Pantoja, C., and Serrano, M. (1998). p19ARF links the tumour suppressor p53 to Ras. Nature *395*, 125-126.

Parisi, T., Pollice, A., Di Cristofano, A., Calabro, V., and La Mantia, G. (2002). Transcriptional regulation of the human tumor suppressor p14(ARF) by E2F1, E2F2, E2F3, and Sp1-like factors. Biochem Biophys Res Commun *291*, 1138-1145.

Park, M.J., Shimizu, K., Nakano, T., Park, Y.B., Kohno, T., Tani, M., and Yokota, J. (2003). Pathogenetic and biologic significance of TP14ARF alterations in nonsmall cell lung carcinoma. Cancer Genet Cytogenet *141*, 5-13.

Petty, E.M., Gibson, L.H., Fountain, J.W., Bolognia, J.L., Yang-Feng, T.L., Housman, D.E., and Bale, A.E. (1993). Molecular definition of a chromosome 9p21 germ-line deletion in a woman

with multiple melanomas and a plexiform neurofibroma: implications for 9p tumor-suppressor gene(s). Am J Hum Genet *53*, 96-104.

Pollock, P.M., Pearson, J.V., and Hayward, N.K. (1996). Compilation of somatic mutations of the CDKN2 gene in human cancers: non-random distribution of base substitutions. Genes Chromosomes Cancer *15*, 77-88.

Pomerantz, J., Schreiber-Agus, N., Liegeois, N.J., Silverman, A., Alland, L., Chin, L., Potes, J., Chen, K., Orlow, I., Lee, H.W.*, et al.* (1998). The Ink4a tumor suppressor gene product, p19Arf, interacts with MDM2 and neutralizes MDM2's inhibition of p53. Cell *92*, 713-723.

Qi, Y., Gregory, M.A., Li, Z., Brousal, J.P., West, K., and Hann, S.R. (2004). p19ARF directly and differentially controls the functions of c-Myc independently of p53. Nature *431*, 712-717.

Quelle, D.E., Cheng, M., Ashmun, R.A., and Sherr, C.J. (1997). Cancer-associated mutations at the INK4a locus cancel cell cycle arrest by p16INK4a but not by the alternative reading frame protein p19ARF. Proc Natl Acad Sci U S A *94*, 669-673.

Quelle, D.E., Zindy, F., Ashmun, R.A., and Sherr, C.J. (1995). Alternative reading frames of the INK4a tumor suppressor gene encode two unrelated proteins capable of inducing cell cycle arrest. Cell *83*, 993-1000.

Roberts, A.B., Anzano, M.A., Lamb, L.C., Smith, J.M., and Sporn, M.B. (1981). New class of transforming growth factors potentiated by epidermal growth factor: isolation from non-neoplastic tissues. Proc Natl Acad Sci U S A *78*, 5339-5343.

Roberts, A.B., Sporn, M.B., Assoian, R.K., Smith, J.M., Roche, N.S., Wakefield, L.M., Heine, U.I., Liotta, L.A., Falanga, V., Kehrl, J.H.*, et al.* (1986). Transforming growth factor type beta:

rapid induction of fibrosis and angiogenesis in vivo and stimulation of collagen formation in vitro. Proc Natl Acad Sci U S A *83*, 4167-4171.

Roberts, A.B., and Wakefield, L.M. (2003). The two faces of transforming growth factor beta in carcinogenesis. Proc Natl Acad Sci U S A *100*, 8621-8623.

Robertson, K.D., and Jones, P.A. (1998). The human ARF cell cycle regulatory gene promoter is a CpG island which can be silenced by DNA methylation and down-regulated by wild-type p53. Mol Cell Biol *18*, 6457-6473.

Saika, S., Saika, S., Liu, C.Y., Azhar, M., Sanford, L.P., Doetschman, T., Gendron, R.L., Kao, C.W., and Kao, W.W. (2001). TGFbeta2 in corneal morphogenesis during mouse embryonic development. Dev Biol *240*, 419-432.

Sanchez-Cespedes, M., Reed, A.L., Buta, M., Wu, L., Westra, W.H., Herman, J.G., Yang, S.C., Jen, J., and Sidransky, D. (1999). Inactivation of the INK4A/ARF locus frequently coexists with TP53 mutations in non-small cell lung cancer. Oncogene *18*, 5843-5849.

Sanford, L.P., Ormsby, I., Gittenberger-de Groot, A.C., Sariola, H., Friedman, R., Boivin, G.P., Cardell, E.L., and Doetschman, T. (1997). TGFbeta2 knockout mice have multiple developmental defects that are non-overlapping with other TGFbeta knockout phenotypes. Development *124*, 2659-2670.

Serrano, M., Hannon, G.J., and Beach, D. (1993). A new regulatory motif in cell-cycle control causing specific inhibition of cyclin D/CDK4. Nature *366*, 704-707.

Sherr, C.J. (2006). Divorcing ARF and p53: an unsettled case. Nat Rev Cancer *6*, 663-673.

Sherr, C.J. (2012). Ink4-Arf locus in cancer and aging. Wiley Interdiscip Rev Dev Biol *1*, 731-741.

Shlyueva, D., Stampfel, G., and Stark, A. (2014). Transcriptional enhancers: from properties to genome-wide predictions. Nat Rev Genet *15*, 272-286.

Silva, R.L., Thornton, J.D., Martin, A.C., Rehg, J.E., Bertwistle, D., Zindy, F., and Skapek, S.X. (2005). Arf-dependent regulation of Pdgf signaling in perivascular cells in the developing mouse eye. EMBO J *24*, 2803-2814.

Spilianakis, C.G., and Flavell, R.A. (2004). Long-range intrachromosomal interactions in the T helper type 2 cytokine locus. Nat Immunol *5*, 1017-1027.

Splinter, E., Grosveld, F., and de Laat, W. (2004). 3C technology: analyzing the spatial organization of genomic loci in vivo. Methods Enzymol *375*, 493-507.

Sporn, M.B., Roberts, A.B., Shull, J.H., Smith, J.M., Ward, J.M., and Sodek, J. (1983). Polypeptide transforming growth factors isolated from bovine sources and used for wound healing in vivo. Science *219*, 1329-1331.

Stone, S., Jiang, P., Dayananth, P., Tavtigian, S.V., Katcher, H., Parry, D., Peters, G., and Kamb, A. (1995). Complex structure and regulation of the P16 (MTS1) locus. Cancer Res *55*, 2988-2994.

Stott, F.J., Bates, S., James, M.C., McConnell, B.B., Starborg, M., Brookes, S., Palmero, I., Ryan, K., Hara, E., Vousden, K.H.*, et al.* (1998). The alternative product from the human CDKN2A locus, p14(ARF), participates in a regulatory feedback loop with p53 and MDM2. EMBO J *17*, 5001-5014.

Tucker, R.F., Shipley, G.D., Moses, H.L., and Holley, R.W. (1984). Growth inhibitor from BSC-1 cells closely related to platelet type beta transforming growth factor. Science *226*, 705-707.

van der Riet, P., Nawroz, H., Hruban, R.H., Corio, R., Tokino, K., Koch, W., and Sidransky, D. (1994). Frequent loss of chromosome 9p21-22 early in head and neck cancer progression. Cancer Res *54*, 1156-1158.

Visel, A., Zhu, Y., May, D., Afzal, V., Gong, E., Attanasio, C., Blow, M.J., Cohen, J.C., Rubin, E.M., and Pennacchio, L.A. (2010). Targeted deletion of the 9p21 non-coding coronary artery disease risk interval in mice. Nature *464*, 409-412.

Wang, Y.C., Lin, R.K., Tan, Y.H., Chen, J.T., Chen, C.Y., and Wang, Y.C. (2005). Wild-type p53 overexpression and its correlation with MDM2 and p14ARF alterations: an alternative pathway to non-small-cell lung cancer. J Clin Oncol *23*, 154-164.

Weber, J.D., Jeffers, J.R., Rehg, J.E., Randle, D.H., Lozano, G., Roussel, M.F., Sherr, C.J., and Zambetti, G.P. (2000). p53-independent functions of the p19(ARF) tumor suppressor. Genes Dev *14*, 2358-2365.

Zhang, Y., Xiong, Y., and Yarbrough, W.G. (1998). ARF promotes MDM2 degradation and stabilizes p53: ARF-INK4a locus deletion impairs both the Rb and p53 tumor suppression pathways. Cell *92*, 725-734.

Zheng, Y., Devitt, C., Liu, J., Mei, J., and Skapek, S.X. (2013). A distant, cis-acting enhancer drives induction of Arf by Tgfbeta in the developing eye. Dev Biol *380*, 49-57.

Zheng, Y., Zhao, Y.D., Gibbons, M., Abramova, T., Chu, P.Y., Ash, J.D., Cunningham, J.M., and Skapek, S.X. (2010). Tgfbeta signaling directly induces Arf promoter remodeling by a mechanism involving Smads 2/3 and p38 MAPK. J Biol Chem *285*, 35654-35664.

Zindy, F., Eischen, C.M., Randle, D.H., Kamijo, T., Cleveland, J.L., Sherr, C.J., and Roussel, M.F. (1998). Myc signaling via the ARF tumor suppressor regulates p53-dependent apoptosis and immortalization. Genes Dev *12*, 2424-2433.

Zindy, F., Williams, R.T., Baudino, T.A., Rehg, J.E., Skapek, S.X., Cleveland, J.L., Roussel, M.F., and Sherr, C.J. (2003). Arf tumor suppressor promoter monitors latent oncogenic signals in vivo. Proc Natl Acad Sci U S A *100*, 15930-15935.